Assessment of the sub-millimeter structure of ice surfaces during ice skating

'Beetje schaatsen; beetje kloten.'

THESIS

submitted in partial fulfillment of the
requirements for the degree of

BACHELOR OF SCIENCE
in
PHYSICS

Author :	Remko Fermin
Student ID :	s1096133
Supervisor :	Tom van der Reep MSc.
	Prof. Dr. Ir. Tjerk Oosterkamp
2^{nd} corrector :	Dr. Daniela Kraft

Leiden, The Netherlands, July 3, 2015

Assessment of the sub-millimeter structure of ice surfaces during ice skating

'Beetje schaatsen; beetje kloten.'

Remko Fermin

Huygens-Kamerlingh Onnes Laboratory, Leiden University
P.O. Box 9500, 2300 RA Leiden, The Netherlands

July 3, 2015

Abstract

An overview of the theoretical work done during the skating project is presented and an upper limit is derived for the presumed water layer under the skate. The skating set-up and its new additions are discussed. It has been found that the ice layer is not flat; it has bumps exceeding the height variations of the skate. The bums disappear during the skating. The bumps in the ice create cavities between the skate and the ice. Simulations indicate the presence of water in these cavities. This was not confirmed because the model used must be extended, to incorporate electrical interactions in the sample. The bumps in the ice layer seem to determine the location and size of the 'shoulders' in the data. These are sudden in- or decrease of the output voltage. The eventual shape of the 'shoulders' seems to be determined by the presence of water in the cavity between the ice and the skate. This to needs to be confirmed in a later stage of the skating project.

Contents

Chapter 1

Introduction

The Dutch have a long marriage with ice skating: as sport, subject of paintings and even transport. One only has to look at a painting of Hendrick Avercamp and it is clear: large plains of ice that are extremely crowded with all sorts of people enjoying 'IJsvermaak'[1] as Avercamp would call it. Another way of finding out how much the Dutch like skating is visiting the Tialf, the fastest ice-track in the Netherlands [1]. Here the national championships are held under the attention of spectators dressed in the most ridiculous orange clothes.

The similarity between the orange skating fans and the people in Avercamp's painting is that both don't know why ice is so slippery. Though it is understandable that the skaters of Avercamp's time have not got any clue, it strange that the contemporaries of the orange wearing skating fans, we, have not either. Especially when we keep in mind that quantum mechanics in more than a century old, and we still do not know why we can skate on ice and not on rubber.

Figure 1.1: *Hendrick Avercamp - 'Winterlandschap met schaatsers', ca. 1608*

[1] This could be translated as: having fun on the ice.

To tackle this question Jorinde van de Vis [2], Tom van der Reep [3], Martijn Zuiddam [4] and Nigel Fennet [5] have sequentially worked on this question as part of their bachelor or master education. The focus in these works has been on finding the presumed water layer under the skate (see chapter 2, Theory). This was however not easy and the data is hard to interpret. Therefore, More insights of the structure of the ice layer are in order. This work will focus on the structure of the ice and will try to answer what influence the thickness variations of the ice layer on the measurements are.

This thesis will be divided in six chapters. After this chapter, a theory chapter is written which contains the theoretical work done during the skating project together with the current theories explaining the low friction coefficient of ice. The third chapter describes the set-up used during the experiments. In the fourth chapter a description of the methods used are discussed, as well as a description of the operation of the MATLAB programs used in processing the data. The results obtained are presented and discussed in chapter five. The conclusions of this thesis are summed up in chapter six. One appendix is included; this appendix is written for future students working on the skating project. In the appendix the measuring procedures using the lock-in amplifier are discussed in detail.

Chapter 2

Theory

This chapter will give an overview of the theoretical models used previously by Van de Vis (section 2.2), Zuiddam (section 2.4) and Van der Reep (section 2.3), as well as a quick overview of the historical most valued theoretical models of the low friction of ice (section 2.1).

2.1 Historical models

The main hypothesis for explaining the low sliding friction of ice-metal contacts, like skating, is the lubrication of the solid ice with water due to melted ice [6]. This idea originated in every day experiences with, for example wet floors [6]. Though plausible, this hypothesis is never tested. This section will give an overview of the hypotheses explaining the cause of the presumed water layer and will conclude with a selection of hypotheses not involving water lubrication.

2.1.1 Pressure melting

In 1886 John Joly referred to the phenomenon of pressure melting as a possible explanation [7]. However, 36 years earlier James Thomson already predicted that the fact that the density of water is higher than that of ice combined with Le Chatelier's principle must mean that the phase transition line between ice and water must have a negative slope [8]. This meant that water freezes at lower temperatures when pressure is applied on the liquid. Joly recognized that this exerted pressure is due to the weight of the skater.

2.1.2 Frictional heating

Much later than Thomson and Joly, in 1939 Frank Bowden formulated a new hypothesis for the cause of the water layer, which is different than pressure melting [9]. This hypothesis formulates that the energy required for melting the ice under the skate is

generated by dissipation of heat under the skate. Bowden pointed out that the pressures that have to be exerted on the ice to create the layer sought after are not realistic. Half a century later Samuel Colbeck added to this hypothesis that skating at temperatures lower than -35°C can not be explained by pressure melting at all [10]. This was studied by attaching a thermocouple to a speedskate.
Pressure melting has more advantages over frictional heating. Pressure melting, at pressures exerted by the mass of a normal person, seems to be only effective in the millidegrees below zero range [11]. Fricional heating does not have this limitation. However, a limitation is that the heat dissipated during skated is absorbed mostly by the skate due to its high heat conductivity. For a further discussion of the thickness of the lubrication layer see section 2.2.

2.1.3 Premelting

The last hypothesis discussed that predicts the cause of the lubricant is premelting. This hypothesis was first formulated by Michael Faraday, in 1850 [6], and is therefore the oldest hypothesis formulated. The premelting hypothesis predicts that there exists a thin layer of quasi-liquid on the ice, independent of the presence of a speed skate. This intrinsic layer supposed to be less than 0.1 μm thick [12]. According to Van de Vis, this layer does not exist when ice temperatures are below -13°C [2]. This means it can not, like pressure melting, be a total explanation for the low friction coefficient of ice surfaces. However it must make a contribution to a presumed water layer since the premelting layer is an intrinsic property of the ice.

2.1.4 Non water lubricated hypotheses

Besides hypotheses involving a presumed water layer other hypotheses have been proposed. This section will give a quick overview of these. Thomas McConica suggested a vapor film exists between the skate and the ice. This film should accommodate the lower friction in a similar way as the water film should [13]. Since the heat transfer in gas is much lower than the heat transfer through liquid the problem of the heat conductivity of the skate, like in Bowden's hypothesis, is no longer a problem [14]. This hypothesis seems to be supported by observations of higher friction between out-gassed metals than their natural counterparts, which contain oxide layers on the surface in which vapor is trapped [14].
Yet a more controversial hypothesis is that of C. Niven [15]. In this hypothesis the molecules on the surface of the ice are used as roller bearings: the skate 'rolls' on top of the molecules like a surface over a series of balls. Whether or not these molecules are part of a quasi-liquid, the molecules have a larger degree of freedom in rotation because not all hydrogen bonds are used[1].
Lastly, Katsutoshi Tusima's adhesion hypothesis can explain the low friction of ice [16] without referring to a lubrication layer. This hypothesis explains the low friction of ice by the fact that the ratio of the adhesive shear strength of the contact area and hardness

[1] In the bulk material of ice the molecules are locked in place because all hydrogen bonds that can be formed, are formed.

is really low. This can explain values of the friction coefficient as low as 0.01 without lubrication.

What is striking is that all above described hypotheses do not seem to conflict with each other. Furthermore, often it is clear that a hypothesis can not explain the entire phenomenon of low friction by itself but hypotheses can collaborate in making a complete picture which covers the phenomenon well.

2.2 Theoretical implementation by Van de Vis

In her bachelor's thesis [2], Van de Vis discussed a hypothesis using the heat equation to simulate the thickness of the presumed water layer created by frictional heating as discussed in section 2.1.2.
Van de Vis solved the heat equation in one dimension analytically and simulates the solution of the heat equation in three dimensions using the program Comsol Multiphysics. A delta function placed in the origin of the coordinate system (r is the distance from the origin) is used to simulate the heat source in the simulations of Van de Vis. The problem to be solved is:

$$\frac{\partial T}{\partial t} = -\alpha \nabla T = \frac{2P\delta(r)}{c_{\text{ice}}\rho_{\text{ice}}} \tag{2.1}$$

In eq. 2.1 T is the temperature of the ice, t denotes time, $\alpha = \frac{k}{c_{\text{ice}}\rho_{\text{ice}}}$ where k is the heat conductivity of the ice, c_{ice} is the heat capacity of the ice, P is the power dissipated per unit area per unit time and finally ρ_{ice} is the mass density of the ice.
Van de Vis shows that this differential equation can be solved in three dimensions as[2]:

$$T = T_0 + \frac{P\delta(r)}{c_{\text{ice}}\rho_{\text{ice}}} \frac{1}{2\pi\alpha r} \left(1 - \text{erf}\frac{r}{2\sqrt{\alpha t}}\right) \tag{2.2}$$

where the parameters are as defined in eq. 2.1. This temperature gradient can be used to calculate a water layer, melted under the skate. In the three dimensional Van de Vis uses an asperity model (based on Herzian contact theory) that describes that 2.6% of the skate is in contact with the ice layer. These asperities have the shape of semi spheres which are melted during contact. Using eq. 2.2 Van de Vis calculated that the frictional heat dissipated can melt away asperities with a radius of 2 μm, this coincides with a water layer of about 1 μm. In the one dimensional case the result was found analytically to be 27 μm, and in simulation to be 3.5 μm. In all the three results a skater with a mass of 80kg was skating with a velocity of 3 m/s on a layer of ice with a temperature of -6°C. The friction coefficient was taken to be 0.02.

2.2.1 Revision of the maximum layer thickness

Now a simpler approach will be made in evaluating Van de Vis' hypothesis. A similar approach will be used: only before and after skating energy considerations are made.

[2]For one dimension, as well as a derivation of the 3D case see [2]

An upper limit of the thickness of the lubrication layer as discussed in section 2.1.2 will be derived in the case of an entirely flat layer of ice and only one point of contact (in the middle of the skate).
Let, as with Van de Vis, the frictional force on the skate be:

$$F_{\text{fric.}} = \mu F_{\text{N}} \tag{2.3}$$

With μ the coefficient of friction and F_{N} the normal force. Then for the energy dissipated per unit time:

$$P_{\text{fric.}} = F_{\text{fric.}} v_{\text{skate}} = \mu F_{\text{N}} v_{\text{skate}} \tag{2.4}$$

with v_{skate} the velocity of the skate. So, after a time period of t seconds:

$$E_{\text{fric.}} = \mu N v_{\text{skate}} t = \mu F_{\text{N}} x_{\text{trav.}} \tag{2.5}$$

of energy is dissipated in the by the frictional force. Where in the second part of eq. 2.5 $x_{\text{trav.}}$ is the distance traveled by the skate. If one assumes that all energy dissipated by the frictional force is transformed into heat which only heats the ice (like in the hypothesis presented by Van de Vis) and the heat travels uniformly trough the ice melting the ice instantaneously, the energy cost of melting a layer of ice with thickness d_{ice} and temperature T (in degrees Celsius) is:

$$E_{\text{melt}} = m_{\text{ice}}(L + c_{\text{ice}}|T|) = \rho_{\text{ice}} V_{\text{ice}}(L + c_{\text{ice}}|T|) = \rho_{\text{ice}} x w d_{\text{ice}}(L + c_{\text{ice}}|T|) \tag{2.6}$$

In eq. 2.6 m_{ice} is the mass of the to be melted ice layer, L is the latent heat of ice[3], c_{ice} is the heat capacity and ρ_{ice} is the mass density of ice[4], w the width of the layer of ice melted (here the width of the skate) and $x_{\text{trav.}}$ the length of the ice layer (here the same as in eq. 2.5).
If the heat conductivity of the skate is zero and no diffusion is happening:

$$E_{\text{melt}} = E_{\text{fric.}} \Leftrightarrow \rho_{\text{ice}} w d_{\text{ice}}(L + c_{\text{ice}}|T|) = \mu F_{\text{N}} \tag{2.7}$$

and from the conservation of mass[5],

$$d_{\text{water}} = \frac{\rho_{\text{ice}}}{\rho_{\text{water}}} d_{\text{ice}} \tag{2.8}$$

then,

$$d_{\text{water}} = \frac{\mu F_{\text{N}}}{w \rho_{\text{water}}(L + c_{\text{ice}}|T|)} \tag{2.9}$$

where in eq. 2.8 and eq. 2.9 ρ_{water} is the mass density of water at the same temperature of the ice. Because not all energy is put in melting the ice and the heat does not travel uniformly through the ice, it is more useful to write:

$$d_{\text{water}} < \frac{\mu m g}{w \rho_{\text{water}}(L + c_{\text{ice}}|T|)} \tag{2.10}$$

[3]Energy needed to melt one kg of ice
[4]$T = 0°\text{C}$
[5]N.B.: This is only the case when the water can only expand in one direction; upwards. No squeeze flow is modeled here.

with g gravitational acceleration, m the mass of the skater and the rest of the parameters as defined above[6]. It may be surprising that eq. 2.10 does not contain a factor v, but μ is dependent on the skate's velocity as $v^{-\frac{1}{2}}$ [2]. This means for the upper limit of the water layer under the skate that for a skater with a mass of m =80 kg, a $\mu = 0.01$ and a skate with a width of 1.1 mm (see section 3.1) on a layer of ice which has a temperature of -6°C:

$$d_{\text{water}} < 20\ \mu\text{m} \tag{2.11}$$

However in the set-up as discussed in chapter 3 used for the experiment a lubricating layer thickness much less than 1 μm is the maximum expected due to lower pressures on the skate.

2.3 Theoretical implementation by Van der Reep

Van der Reep based the theory part in his master's thesis [3] on a series of papers published by Lozowski and Szilder[7]: the hydrodynamic model. This model considers circularly curved skate which cuts through and sinks in the ice by melting it away. In principle this is a more extended model of that of Van de Vis but taking in account not only frictional heating, but also premelting and pressure melting. Furthermore, this model also incorporates the squeeze flow of water from under the skate to the sides. Lozowski and Szilder derive a differential equation which describes the forming of the water layer along the skate's length (measured in x; total length of the skate is l):

$$\frac{\partial d_{\text{water}}}{\partial x} = \frac{\mu_{\text{visc.}} v}{d_{\text{water}} \rho_{\text{water}} L} - \frac{k \Delta T_{\text{b}}}{d_{\text{ice tot.}} v \rho_{\text{water}} L} - \frac{k \Delta T_{\text{i}}}{\rho_{\text{water}} L \sqrt{\pi \kappa_{\text{ice}} v x}} - \frac{2 m g d_{\text{water}}}{3 \beta \mu l w w_{\text{t}}^2 v} \tag{2.12}$$

with,

$$\beta = 1 - \frac{8}{3 w w_{\text{t}}^2} \left(\frac{w_{\text{t}}}{2} - w_{\text{s}} \right)^3 \tag{2.13}$$

The first term in eq. 2.12 is the term governed by the melting of the ice. In this term $\mu_{\text{visc.}}$ is the viscosity of the water. The other parameters are as defined above in section 2.2. This holds for the other terms as well. In the second term ΔT_{b} is the temperature difference between the bottom of the ice layer and the top of the ice layer and $d_{\text{ice tot.}}$ is the thickness of the ice layer[8].
The second and the third term describe heat conduction but because they both contain instantaneous melting temperatures[9] Besides, they both describe pressure melting. In the third term κ is the thermal diffusivity of the ice. T_{i} is the difference between instantaneous melting temperature in the case of applied pressure and in the case of no applied pressure.
The fourth and last term is determined by the squeeze flow. of water to the sides of the skate. Most terms are already introduced in this section or in section 2.2, but w_{t} is the

[6] N.B.: eq. 2.6 to eq. 2.10 must be read in S.I. units, except for the temperature which must be read in degrees Celsius.

[7] The papers discussed are: [17] [18] [19]

[8] N.B.: not the thickness of the melted ice layer as in section 2.2.1

[9] In the second term the temperature of the top of the ice layer is the instantaneous melting temperature in the third term it is hidden in T_{i}.

total length over which the skate is in contact with the ice measured in the direction perpendicular to the direction of motion, so:

$$w_t = w + 2w_s \tag{2.14}$$

where w_s is the track depth of the skate. In this hypothesis the skate makes contact with the ice on the sides of the skate. The parameters in eq. 2.13 are the same as introduced above.
Eq. 2.12 has a singularity in $(x, d_{water}) = (0, 0)$. This singularity is resolved by assuming a small initial value for both parameters, the ice layer contains a lubricating layer before the skate has even passed. This can be interpreted as the premelting layer, according to Van der Reep.

Using this hypothesis, Van der Reep makes some predictions about the thickness of presumed water layer. For a skater weighing 80 kg skating at a velocity of 1 m/s on a ice layer of $-5°C$, the lubricating water layer would be 18 nm. However in the conditions used during experiments a layer thickness of 7 nm is more likely. Striking is that the values for the layer thickness are hypothesized much smaller, they do not exceed the micro meter scale. This is caused mainly by the squeeze flow, which is not present in the theoretical expressions of Van de Vis.

2.4 Theoretical implementation by Zuiddam

This section will give brief a description of the measuring technique developed by Zuiddam described in his bachelor's thesis [4]. This is presented as theory because the technique does not function yet on the current set-up. Zuiddam made use of the fact that the relative permittivity of ice is strongly frequency dependent. This implies that if during a passage of the skate in the set-up as described described in chapter 3, measurements took place with a 11 kHz and 1 MHz signal, then visually, an lubricating water layer could be detected as well as by plotting the ratio of the capacitances found during the experiments with different frequencies (ratio of eq. 3.5 with different frequencies), see figure 2.1.

According to Zuiddam the flat surface in the data could be interpreted as a water layer under the skate. Zuiddam also rightfully noted that the forth and back peaks in his experiment are symmetric, this tells us that skating the presumed water layer could be symmetrically formed under the skate.
Though non-realistic values were obtained for the air thickness under the skate, this is a promising method for evaluating the lubricating layer thickness under the skate.

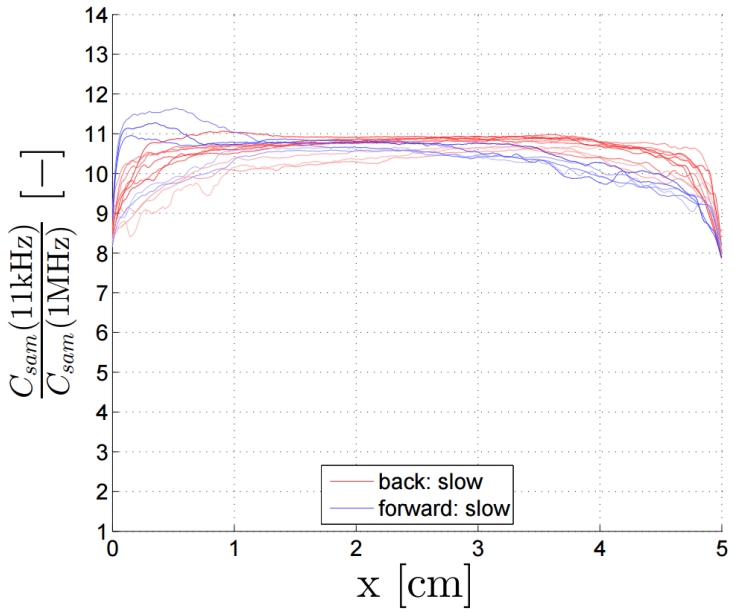

Figure 2.1: *A plot of the ratio of capacitances as function of the length of the skate, found during an experiment done by Zuiddam. The flat area in the middle of the skate can indicate a water layer being stuck to the skate due to capillary forces.*

2.5 Conclusion

There are multiple hypotheses that explain the low friction coefficient of ice; the most prominent of them involve a lubricating water layer between the skate and the ice layer. An upper bound has been derived for water under the skate: in typical conditions the maximum thickness of the water layer caused by frictional heating should not exceed 20 μm. In the experiments on the set-up as described in chapter 3 values exceeding 1 μm will not be observed. However Van de Vis derived analytically a layer thickness of 27 μm, but a thickness of 3.5 μm in simulations; both in the 1D case and in the case of a real skating situation. In the three dimensional problem she derived a layer thickness of about 1μm. Van der Reep on the other hand found values of the lubricating layer thickness much smaller. 18 nm in the case of a real skater. From theory we can conclude that a lubrication layer, caused by a combination of processes, with a thickness between 10 nm and 1 μm is the most favored explanation for the low friction coefficient of ice.

Chapter 3

Set-up

This chapter in section 3.1 will give an brief overview of the current set-up as built by Fennet[5], as well as a more detailed overview of the new additions made. The latter consists of the dial gauge (section 3.4), the new skate track (section 3.3) and the force sensor (section 3.5).

3.1 Overview of the current set-up

The current set-up will now be described from bottom to top. On the bottom the set-up a thermoelectric cooler (TE Technology CP- 121), based on the peltier effect (part 10 in figure 3.1) resides. This cooler extracts heat from the top of the set-up and uses fans to transport this heat away from the set-up.
On the thermoelectric cooler a large perspex box rests in which a low humidity atmosphere is created for the protection of of the set-up. This way no water vapor can condensate on the set-up; this causes the electronics to short-circuit. The other reason for using this shielding gas is making sure the possible water layer caused by skating, which is to be measured, is not contaminated by condensation water.
In the covering box one can find the electronics for processing the data of the skate, the skate track (see section 3.3) and the servo motor to drive the skate or dial gauge (part 7 in figure 3.1). The electronics and the skate track are built on a printed circuit board (PCB); depicted as part 9 in figure 3.1.

The servo motor (model: RCP4-SA5C-I-42P ROBO Cylinder [5]) is capable of moving a mass along an axis with speeds ranging between 0.01 mm/s and 1440 mm/s. the acceleration can be set from 0.01 g to 1 g. On the servo two different systems can be mounted. Firstly, the skating system (parts 1 to 6 in figure 3.1) and secondly the dial gauge system (see section 3.4). The skating system is consisting of a stainless steel holder in which the skate is set in place (part 4 in figure 3.1). The skate is connected to the holder by the force sensor (see section 3.5). The holder can be pressed down, using air pressure, to simulate the mass pushing down on the skate. The air pressure is applied on a piston with a diameter of 12 mm (part 3 in figure 3.1). This means 1 bar of pressure coincides with 11.3 N of force or 1.15 kg of mass pushing down on the skate.

The minimum force applied on the skate is 0 N, the maximum is around 3.5 bar[1]. The skate can be rotated horizontally with respect to the direction of movement by setting adjusting screws at the sides of the holder (part 5 in figure 3.1). The skate is allowed to rotate freely along the axis perpendicular to the axis of movement to simulate the ankle joints in a human being and to make sure the skate is placed directly on the ice, even under a constant ice thickness in- or decrease. For an overview of the set-up see figure 3.1.

The skate used, is a model of a real skate scaled down to 5 cm in length and 1.1 mm in width (part 6 in figure 3.1). It is curved with a radius of 22 meters, as real speed skates are, and is rounded at the edges.

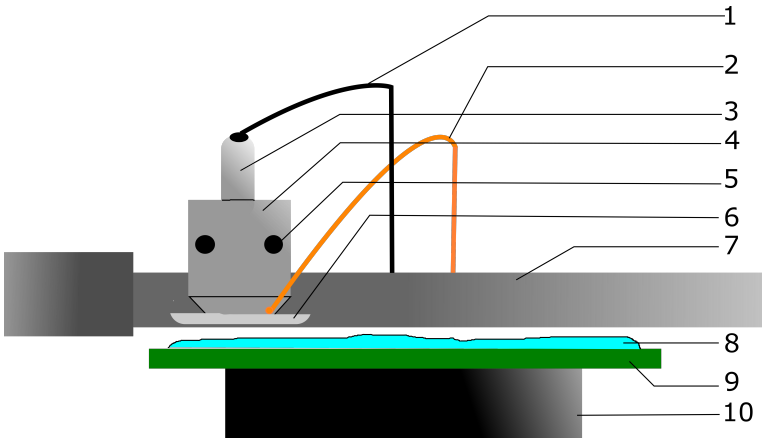

Figure 3.1: *A general schematic overview of the current set-up. Parts 1 to 6 are the skating system (for the dial gauge system see figure 3.3; for close-up of the skating system see figure 3.4(a)). Part 1 is the air-pressured cable, which is connected to part 3 in which the piston is transforming the pressure to force to simulate the weight of the skater. Part 4 is the skate holder under which the skate is placed (part 6). The skate is connected to the lock-in using the cable depicted as part 2. The angle between the axis of motion and the skate can be adjusted using part 5: the adjusting screws. The skating system is mounted on the servo (part 7). Part 8 is the ice layer and part 9 is the PCB, which are resting on the thermoelectric cooler (part 10). The perspex box of the set-up is not drawn here.*

3.2 The electronics and transfer function

The signal send to the skate to determine the capacitance of the dielectric, is provided by a Zurich instruments HF2LI lock-in amplifier. After passing the skate the signal is picked-up by the electrodes and the current that passes through the dielectric is converted to an output voltage, by an IV-converter. The output voltage is then send to the lock-in amplifier. Here it is processed and saved[2]. For a broader description of the lock-in amplifier see appendix A; a description of the functions of the lock-in written for the students who will work on the skating project in the future. For an overview of the electronics see figure 3.2.

[1] It is possible to increase the pressure further but the ice breaks approximately at this pressure.
[2] All files are saved on the universities 'data01' server in the folder 'ip/Remko'.

Van de Vis and later Van der Reep calculated the transfer function of the set-up. The electronics have not changed during the rebuilding of the set-up by Fennet except for two attributes: the type of operational amplifier (opamp) used and the type of cable between the electrodes and the IV-converter. The old opamp used was a Burr-Brown OPA 657, this is replaced by an Burr-Brown OPA 656u. Fennet also changed the type of wiring between the electrodes and the IV-converter: the flat cable previously used on the set-up is discarded and the wiring is incorporated in the PCB. This reduced the cable capacitance, C_C, substantially causing the noise to drop. Besides, the rebuilt of the PCB means that the resistors used have smaller spatial dimensions than the old ones; this caused a drop in parasitic capacitance.

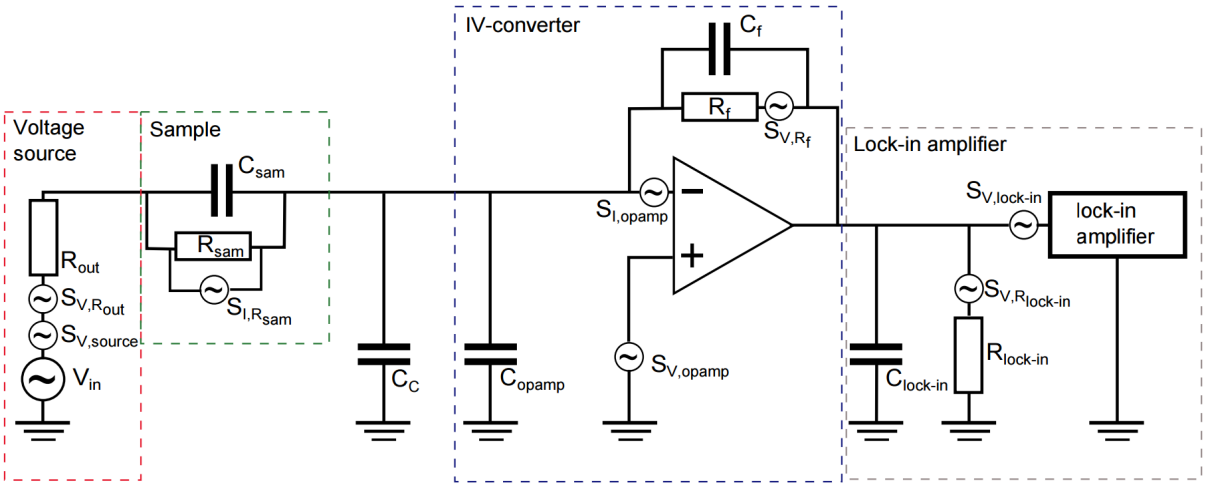

Figure 3.2: *A schematic overview of the electronics. In the experiments done, the voltage source is the lock-in amplifier. The skate and electrode are depicted with 'sample'. As mentioned in the text, the C_C has been lowered drastically by incorporating the cable in the PCB. Figure kindly supplied by Van der Reep[3].*

3.2.1 The transfer function

Now the transfer function, as calculated by Van der Reep, will be presented[3]:

$$H = \frac{V_{in}}{V_{out}} = -\frac{1}{\sqrt{2}(1+q)} \frac{Z_f}{R_{out} + Z_{sam}} \text{ where } |q| < 1 \tag{3.1}$$

where,

$$q = \frac{Z_f}{G} \imath\omega (C_C + C_{in,opamp}) \tag{3.2}$$

and,

$$Z_f = \frac{R_f}{1 + \imath\omega R_f C_f} \tag{3.3}$$

and finally,

$$Z_{sam} = \frac{R_{sam}}{1 + \imath\omega R_{sam} C_{sam}} \approx \frac{1}{\imath\omega C_{sam}} \tag{3.4}$$

[3]For derivation of the transfer function, see [3]

In eq. 3.4 formulas Z_f denotes the impedance of the feedback loop (RC-filter due to parasitic capacity of the resistor), Z_{sam} is the impedance of the sample and q is a recurring factor in the derivation of the transfer function. In eq. 3.2 G is the gain of the opamp. R_{out} and R_f symbolize the resistance between the voltage source and the sample and the resistance in the feedback loop. The same for R_{sam} which is the resistance of the sample. C is capacitance; the same subscripts hold for capacitance as for resistance. Generally, ω denotes a the angular frequency of the input signal and $\imath$ denotes the imaginary number. The factor $1/\sqrt{2}$ is caused by the lock-in amplifier which has a read out in a rood-mean-squared voltage.

The transfer function can be used to determine the capacitance of the the sample; one can write eq. 3.1 as:

$$\frac{1}{C_{sam}^2} = \omega^2 \left(\left| \frac{Z_f V_{in}}{\sqrt{2}(1+q)V_{out}} \right|^2 - R_{out}^2 \right) \tag{3.5}$$

with V_{in} and V_{out} respectively the in- and output voltage and other symbols as introduced above.

3.2.2 Noise

The electrical noise spectrum of the set-up was predicted by Van de Vis and Van der Reep alongside of their prediction of the transfer function. Again only the results of Van der Reep are presented. The electrical noise of the set-up is caused by thermal voltage noise in the resistors in the circuit of figure 3.2, as well as thermal current noise in the sample. Other noise sources are lock-in amplifier voltage noise, opamp voltage noise, opamp current noise and noise resulting from the source of the signal (lock-in). The total noise spectrum is given by:

$$\begin{aligned} S_{tot} =& S_{V,R_{out}} |H|^2 + \frac{1}{2}\frac{1}{(1+q)^2} S_{I,R_{sam}} |Z_f|^2 + \frac{1}{2}\frac{1}{(1+q)^2} S_{V,opamp} \left| H_{opamp} \right|^2 + \\ & \frac{1}{2}\frac{1}{(1+q)^2} S_{V,R_f} + \frac{1}{(1+q)^2} S_{V,R_{in}} + \frac{1}{(1+q)^2} S_{V,lock\text{-}in} + S_{V,source} |H|^2 \end{aligned} \tag{3.6}$$

In eq. 3.6 H, Z_f and q are as defined above in section 3.2.1. The factor $\frac{1}{2}$ stems from the rms readout of the lock-in amplifier. Furthermore, $S_{V,R_{out}}$, S_{V,R_f}, $S_{V,R_{in}}$ and $S_{I,R_{sam}}$ denote thermal Johnson voltage and current noise respectively:

$$S_{V,R} = 4k_b T R, \quad S_{I,R} = \frac{4k_b T}{R} \tag{3.7}$$

with temperatures T either room temperature or the temperature of the sample and the resistance R the designated resistance (depending on the parts of the set-up). k_b is

the Boltzmann constant. $S_{\text{V,opamp}}$ and $S_{\text{V,lock-in}}$ in eq. 3.6 are the noise spectra of the opamp and the lock-in. These are given by:

$$S_{\text{V,x}}(\omega) = S_{\text{V, x}}(\infty)\left(1 + \frac{\omega_{\text{c,x}}}{\omega}\right)^{-2} \tag{3.8}$$

with the x representing opamp or lock-in. Here ω_{c} is the cut-off radial frequency of the corresponding noise spectrum. $S_{\text{V,source}}$ is the noise spectrum caused by the source of the signal. Finally, H_{opamp} is the transfer function of the IV-converter and is given by:

$$H_{\text{opamp}} = \frac{1}{\frac{1}{G} + 1 + \imath\omega Z_{\text{f}}(C_{\text{C}} + C_{\text{in,opamp}})} \tag{3.9}$$

with G the opamp gain, as defined as above. The same holds for other parameters.
The noise caused by vibrations of the servo are negligible when measuring at the high frequencies, at which the experiment is conducted (see section 4.2), according to Fennet[4]. In the spectrum no 50Hz components are visible due to the placing of ferrite rings in the wiring of the set-up.

3.2.3 Changed parameter values

Since a few components in the set-up are changed during the rebuild of the set-up a couple of parameters changed along side. This subsection will give an overview of the changed parameters with respect to the parameters as presented by Van der Reep [3][5]. The changed parameters are presented with there source in table 3.1.

Table 3.1: *An overview of all the parameters that have been changed due to the rebuilt of the set-up by Fennet. All symbols are as defined in section 3.2.1. Here f denotes the frequency of the input-signal and f_{c} is an cut-of frequency of the matching property.*

Parameter	Symbol	Magnitude	Source
Cable capacitance	C_{C}	6 pF	Fit
Opamp gain	G	$10^{3.25}\left(1 + \frac{\imath f}{f_{\text{c}}}\right)^{-1}$ with $f_{\text{c}} = 10^{5.0}$ Hz	[20]
Opamp current noise density	$S_{\text{I,opamp}}$	1.3 $\frac{\text{fA}^2}{\text{Hz}}$	[20]
Opamp coltage noise density	$S_{\text{V,opamp}}$	$7.0\left(1 + \frac{f_{\text{c}}}{f}\right)^2$ $\frac{\text{nV}^2}{\text{Hz}}$ with $f_{\text{c}} = 10^{5.0}$ Hz	[20]
Feedback capacitance	C_{f}	80 fF	Fit

The parasitic capacitance in the feedback-loop is adjusted to better fit the data. This is justified by the fact the new resistors have less big spatial dimensions than the ones used in the old PCB. The feedback capacitance is almost halved.

[4]From personal communications.
[5]The rest of the parameters used during simulations can be found on page 14 of [3].

3.3 The skate track

During this experiment two types of skate track are used. Firstly the old track, installed by Fennet, and secondly the new track which contained improvements to create more flat ice. The skate track is situated on the PCB between the servo and the electronics' housing. It consists of 16 electrodes[6] on which a layer of 25.4 μm thick kapton tape is placed. The old track was 20 cm long and 0.4 cm wide and is bounded by regular tape. The new track is as long as the old track but is more wide: the width is 1.4 cm. furthermore, the kapton tape layer is covered with a layer of mica. Mica is hydrophilic as opposed to kapton which is hydrophobic. Besides, mica is quite permeable for water. This required an additional layer of teflon tape to be put along the edges of the mica. The teflon tape and the mica are stuck in place by applying regular tape as in the old skating track. Both the increased width and the change in polarization of the substrate on which the ice is grown should decrease the height variations in the ice layer.

3.4 The dial gauge

The dial gauge system is built to better understand the structure of the surface of the ice layer. The model of dial gauge that is used is a Garant 43 2110_IO/58; this device mechanically probes the surface of the ice layer and shows the height of the ice layer.

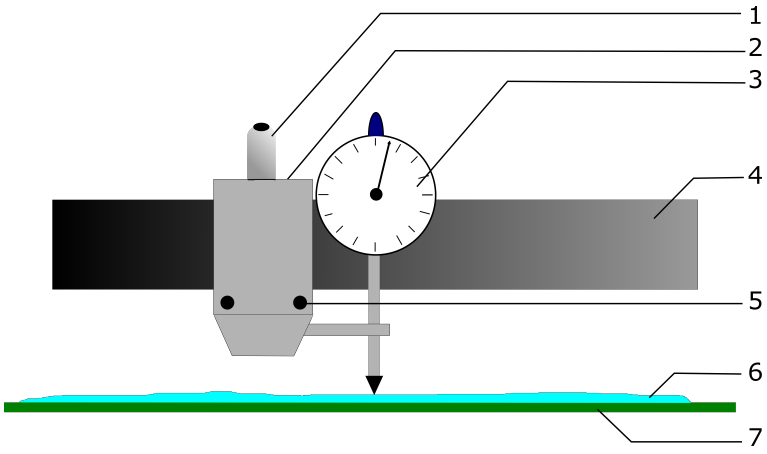

Figure 3.3: *A Schematic figure of the dial gauge system. Part 1 is the air piston Part 2 is the old skate-holder which is reused for keeping the dial gauge in place. The two adjusting screws can are depicted as black circles (part 5). Part 3 is the dial gauge as described in the text. Part 4 is the servo (not entirely drawn). Part 6 is the ice layer and part 7 is the PCB. As can be seen, the dial gauge can be moved along the skating-track and evaluate the ice thickness at pre-set positions. The thermoetric cooler, the mailman elastics and the perspex box are not drawn.*

The dial gauge's measuring 'ticks' are 10 μm apart. For making reproducible measurements the dial gauge needs to be attached firmly to the servo. This is done by attaching it to an old skate holder (a new one is built to incorporate the force sensor; see section

[6] 13 small circular ones with $A = 1.7 * 10^{-7}$ mm^2 and 3 larger rectangular ones having rounded edges with $A = 38 * 10^{-7}$ mm^2.

3.5). The skate holder is held in place in a constant position by dutch mailman elastics, which are strapped around the, in this measurement system, obsolete adjusting screws and the air pressure piston (respectively parts five and one in figure 3.3).

3.5 The force sensor

Direct force measurements were not possible in the past, but information of the frictional forces can bring a great insight in what is happening underneath the skate. This is the reason a sensor is built on the set-up[7].

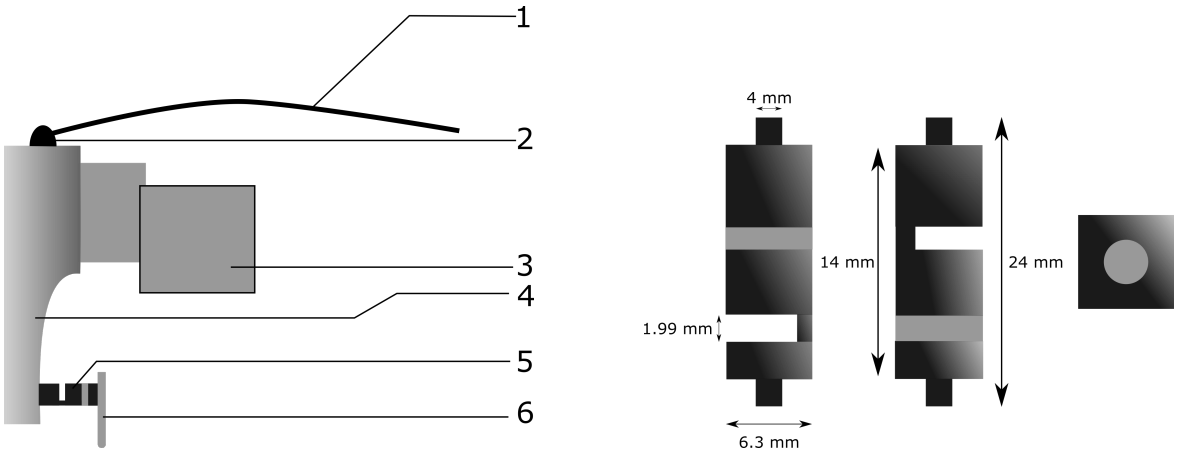

(a) *A schematic close-up of front view the holder in the skating system. The holder (part 4) is placed on the servo (part 3) and pushed down using the piston (part 2) which is supplied by the air-pressured cable (part 1). The skate (part 6) is connected to the holder by the force sensor depicted by part 5. The adjusting screws are not drawn here.*

(b) *The force sensor in schematic close up (part 5 in figure a). The left and the middle drawings are front views of the sensor; the right is one from the top (the bottom view is exactly similar and therefore not shown). The middle drawing is rotated ninety degrees counterclockwise along the length axis of the sensor. This figure is not true to scale.*

Figure 3.4: *A schematic close-up of the skating system (a) and a schematic close-up of the force sensor (b).*

The force sensor is supplied by Strain Measurement Devices and is named x,y-joystick sensor (see figure 3.4(b)). It is built out of stainless steel 24 mm long and 6.3 mm wide which is cut out in two places, so two cavities remain. The sensor can, due to an applied force and torque, bent in these regions. Furthermore, this changes the electrical properties of the material. From this a force is derived. Since force can be measured in two directions it is possible to measure the normal force and the frictional force at the same time. These two forces can be used to calculate the frictional coefficient.
The sensor is supplied by an voltage source of 5 V, which is applied over both the cavities in the sensor. The output of the sensor is a thousand times lower than the input, this means an amplification is in order to produce a signal, which can be properly digitized. The amplification is done by an instrument amplifier which amplifies the signal

[7]The sensor is installed on the skate set-up and provided with the necessary amplification equipment. No measurements are conducted yet at the time of writing due to time shortage.

201 times. The readout is done by either the lock-in amplifier or a data acquisition box (DAQ box)[8].
The sensor is placed between the skate and the skate holder. Due to the dimensions of the sensor a new holder is built to ensure spacial dimensions are no problem (see figure 3.4(a)). Calibration data will have to be obtained before measuring forces are possible.

[8]N.B.: At the time of writing no suitable DAQ box is made available yet. This has to be done in the future.

Chapter 4

Methods

This chapter will give an overview of the methods used during measurements of the ice thickness. When conducting a measurement there are two methods recognisable. Firstly, measuring the height of the ice layer using the dial gauge (discussed in section 4.1). The second method is the measurement technique firstly described by Van der Reep [3]. The latter is a measurement of the capacitance of the ice layer, from which the thickness of the ice layer as well as the thickness of the possible water layer on the ice, can be measured (discussed in section 4.2). Finally, the operation of the different MATLAB programs is discussed in section 4.3.

4.1 Growing ice and measurements using the dial gauge

A typical measurement starts with growing ice. This is done with about one milliliter (1 ± 0.2 ml) of demineralized water, that is placed using a pipette on the ice-track. The peltier freezes the water, which results in a ice layer with a thickness between 100 μm and 400 μm. The water is frozen for over one hour the ensure the water is properly frozen and the ice reaches thermal equilibrium.

After the freezing the ice is ready for skating. First the thickness of the ice is assessed using the dial gauge. The dial gauge is mounted on its carrier on the servo at the beginning of the ice-track ($x_{\text{dial gauge}} = 0$ mm) so the the dial gauge's deviation is zero micrometers[1]. The servo is then used to place the dial gauge at pre-set positions on the ice to measure the ice layer thickness. The latter is done with increments of 1 mm with a velocity of $v_{\text{dial gauge}} = 1$ mm/s. The data is obtained manually and later processed in Origin Pro (64 bit).
The precision of the dial gauge is 10 μm but the to 1 μm the thickness can be estimated. The error on the measurements is taken to be a minimum of 5 μm. After measuring the ice thickness the servo is moved to the starting point of the track; the readout on the dial gauge determined the error on the just finished measurement. Theoretically

[1] N.B.: before doing measurements on ice the deviations of the thickness of the kapton tape surface of the PCB are assessed. Later the thickness of the ice layer is corrected to only incorporate the ice thickness. The thickness of the mica is not assessed however, due to the softness of the material.

this readout should be zero, if it is not, the error is taken to be the the value of the dial gauge at $x_{\text{dial gauge}} = 0$ mm[2].

4.2 skating measurements

After concluding the measurements using the dial gauge, the dial gauge is removed from its holder on the servo and replaced by the skate. Sequentially the skate is pushed down on the PCB to ensure the skate is placed properly straight[3]. After this, the skate is placed on the ice at the beginning of the track at $x_{skate} = 90$ mm and the pressure is applied to simulate the mass pushing on the skate. Next the the voltage is applied on the skate and the IV-converter[4].
Skating is done between pre-set points on the skating track. Typically this is between $x_{\text{skate}} = 90$ mm and $x_{\text{skate}} = 180$ mm. The data obtained during skating is saved in sets of ten times forth and back (twenty times passing the electrode). Generally this is repeated ten times (in total: 100 times back and forth or 200 times passing the electrodes). After skating, the skate is removed from the servo and the dial gauge is set in place and the dial gauge measurement routine is repeated.

the typical speeds at which the skating measurements are conducted are $v_{\text{skate}} = 50$ mm/s or $v_{\text{skate}} = 100$ mm/s, though exceptionally low speeds of $v_{\text{skate}} = 1$ mm/s or $v_{\text{skate}} = 10$ mm/s and high speeds of $v_{\text{skate}} = 200$ mm/s are used.
The maximum acceleration of 1 g is used to ensure the skate moved with the right speed before reaching the electrode. The typical pressure used is $p = 0.3$ bar (this equals $m = 345$ g). Higher pressures that are sometimes applied ranged between $p = 1.0$ bar and $p = 1.5$ bar (respectively $m = 1.15$ kg and $m = 1.73$ kg). The reason for using low pressures is protecting the force sensor for overloading.
The ice temperature is kept constant at $T = -18^{\circ}$C[5]. All measurements are conducted using electrodes[6] 9 en 10 placed at respectively $x_{\text{dial gauge}} = 106$ mm and $x_{\text{dial gauge}} = 118$ mm. All measurements are conducted with the skate pointed parallel to the direction of movement.

The lock-in amplifier produced the input signal for the skating measurements. Due to the limitation of the number inputs in the lock-in, it is possible to measure the two electrodes at the same time or measure at one electrode with two input signals. Because using two electrodes at the same time is producing a better insight in the structure of the ice layer and the $f = 11$ kHz measurements are quite noisy, using one frequency of $f = 1$ MHz is the preferred method. For a broader description of the use of the lock-in amplifier see appendix A.

[2]N.B.: unless the readout is less than 5 μm; the minimum error.
[3]This is done at $x_{\text{skate}} = 0$ mm, this means $x_{\text{dial gauge}} = -78$ mm.
[4]N.B.: the voltage on the skate and IV-converter are switched off during dial gauge measurements.
[5]The voltage source is set to produce a constant current of $I = 8.5$ A. This corresponds to the above mentioned temperature according to Van der Reep, see [3] appendix D.
[6]These are small electrodes.

4.3 Processing data

The raw data, being ZIBIN files, is processed using a second version Van der Reep's program *TTAnalysis_ziLoad.m*[7] which is adapted for the mechanized experiment. This program is used to convert the raw data in averaged voltage peaks. This averaging is done per ten passages and is done skating forth and separately from skating back. These outputs are used in the newly written program *Compare_signal_characteristics.m*; a program developed to study the behavior of the maximum averaged output signal. For making a connection between the dial gauge data and capacitive data a program is written, *AirLayerSkate.m*, which places a simulated skate on the measured ice layer [8]. *Set-up.m*, a program written by Van der Reep, is used for producing a prediction of the signal as function of the frequency of the input signal (frequency sweep), as well as a prediction of the noise spectrum and of the signal during a passage of the skate. The attentive reader may have already noticed this from the file format of the programs, but the programs discussed in this section are all written in MATLAB 2014b (64bits). Below follows a description of the programs used for processing the data and making predictions of the expected data.

4.3.1 The program *AirLayerSkate.m*

After acquiring the dial gauge data, a need existed for further processing the data. To accommodate this need AirLayerSkate.m is written. The program simulates the placing of a virtual skate on the measured ice layer data.
For this purpose firstly, the dial gauge data is loaded which is saved as CSV format. Next the user determined a few settings: the initial height of the to be created virtual skate, the position of the electrode in the ice layer and the steps in which the skate is tuned during fine tuning (angle of attack and steps of lowering the skate). Finally, the user is asked to determine on which locations of the ice layer the skate should be lowered. The indicated points are taken to be the left end of the skate. This means that if the skate should be placed at x than the skate is built from x to $x + 5$ cm.

Because it is not always possible to make use of a dial gauge data-set which covers the entire ice-tack, the program would next built the skate, x-axis and the ice layer at the possible locations. The skate is constructed floating over the ice with an initial height (with respect to the bottom of the ice layer) as determined earlier by the user. The skate and ice layer are next plotted together with an indication of the location of the electrode (see figure 4.1).

Now the virtual skate is ready to be lowered on the ice layer. For this purpose the skate is first twisted as approximation. This is done by finding the highest point in the ice layer on the left of the center of the skate as well as on the right. Since the skate must be supported by at least two points (one left of the center; one right) to be stable,

[7] For a broader description of Van der Reep's program see [3] appendix C. N.B.: this program was written for the manually driven experiment.
[8] Measured using the dial gauge.

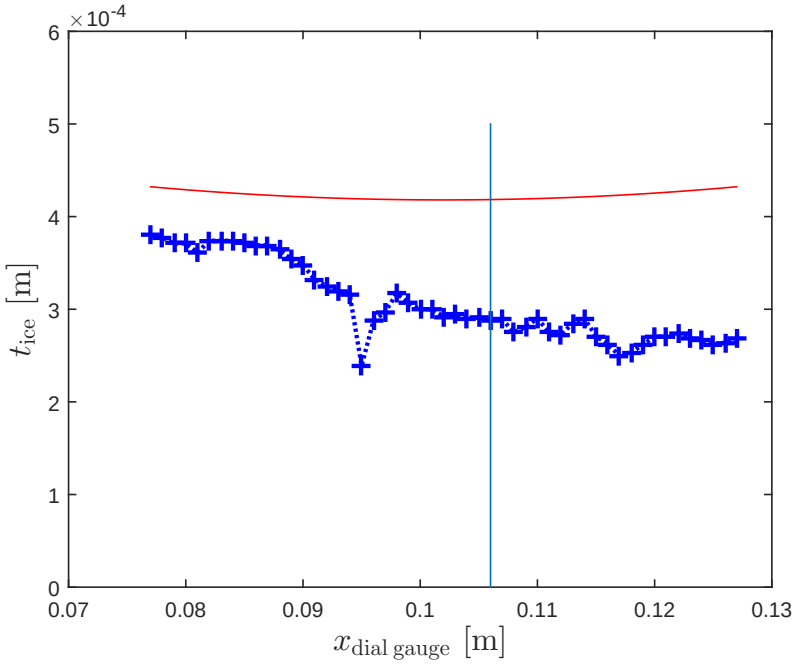

Figure 4.1: *Plot of the first step of the simulation using AirLayerSkate.m. In red the skate is plotted above obtained gauge dial data (blue). The light blue vertical line indicates the position of the electrode under the ice.*

the approximation of the angle of attack of the skate is:

$$\alpha_{\text{approximation}} = \arctan \frac{d_{\text{max,left}} - d_{\text{max,right}}}{x_{\text{max,right}} - x_{\text{max,left}}} \tag{4.1}$$

where $d_{\text{max,left}}$ is the thickness of the ice at the highest point under the left side of the skate; $d_{\text{max,right}}$ the same for the highest point under the right side. $x_{\text{max,left}}$ and $x_{\text{max,right}}$ are the locations of the above mentioned points.
Now the skate is ready to be rotated and lowered resulting in the plot in figure 4.2(a).

As can be seen in figure 4.2(a) is the skate not properly placed on the ice. The program now checks whether on the left and right side of the skate the skate is supported. If the skate is not supported on the left side of the center it is rotated counter-clockwise over an angle $\Delta\alpha$ as defined by the user in the top of the program. The skate is rotated $15\Delta\alpha$ if the left side of the skate is more than 10 micrometer above the ice. The same is done clockwise if the skate is not supported on the right side of the center.
Next the skate is lowered carefully with increments as indicated by the user in the beginning of the program. if the skate touched the ice on either the left or the right side of the center rotations are done again. This continued until the skate is supported on both the right side of the center and the left side of the center (see figure 4.2(b)).
If the program did not finish fine tuning before a fixed number of iterations (rotations), the program would terminate.

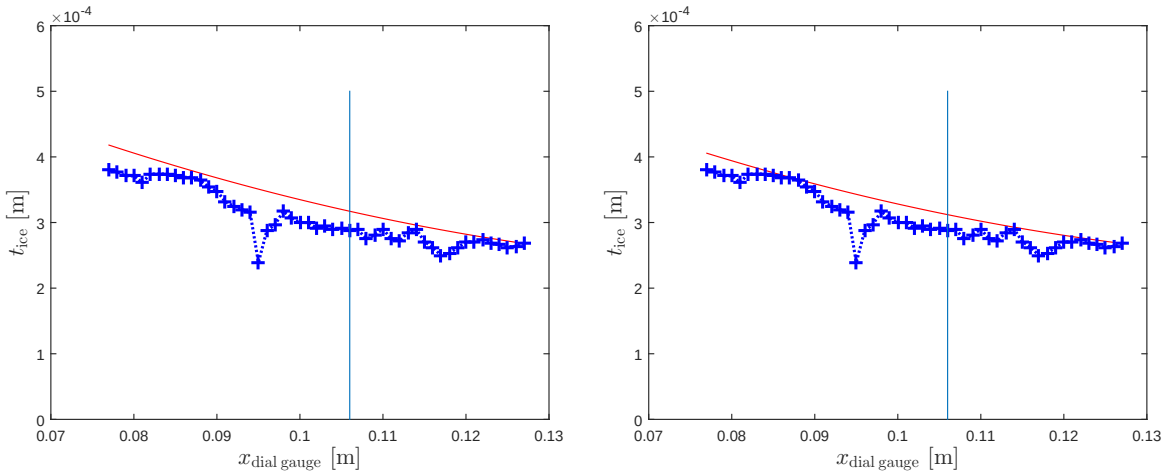

(a) *The second step of the simulation of AirLayerSkate. The skate is lowered on the ice and seems to be in the right place. However, under closer inspection one can see the skate is not properly supported by the ice.*

(b) *The third and last step of the simulation of AirLayerSkate. After finetuning the skate is properly supported by the ice. This means the weight of the skate is devided over at least two peaks in the ice.*

Figure 4.2: *The last two steps in the simulation of the lowering the skate on the ice using AirLayerSkate.m. The plots represent the same entities as in 4.1*

The final step after fine tuning is calculating the difference between the skate and the ice layer. This result is saved for use in the program Set-up.m (see section 4.3.2). Next the entire process is repeated for a new location of the skate. If possible the to be evaluated locations are $x_{\text{electrode}} - 5$ cm to $x_{\text{electrode}}$.

4.3.2 the program *TTAnalysis_ziLoad.m* and *Set-up.m*

As mentioned above the MATLAB code *TTAnalysis_ziLoad.m's* main used output is the average signal. Before making this output, the program first loads the raw data: a time trace with multiple (most of the measurements: 20) peaks. After this, the program selects these peaks from the time trace[9], saves them separately and makes them all of equal length by linear interpolation of the data points. After this, the peaks are divided in peaks skating back and skating forth, by using a counter. Odd peaks are forth, even are back[10]. The peaks are averaged next per time trace and direction (typically ten per measurement per direction).

The program Set-up.m functions as the title suggests: it can predict frequency sweep data (the output voltage of the set-up as function of frequency) or predict the output of the set-up during a passage of the skate. Besides, it can make a prediction of the spectrum of the noise. All calculations are based on the theory discussed in chapter 3.

To use the data obtained by AirLayerSkate.m and make the connection with the capacitance measurements, the calculated thickness of the presumed air layer between

[9] This is done on basis of a signal amplitude above a set voltage and set length

[10] The skate is by placed left of the electrode before measurements could start. so forth is always from left to right.

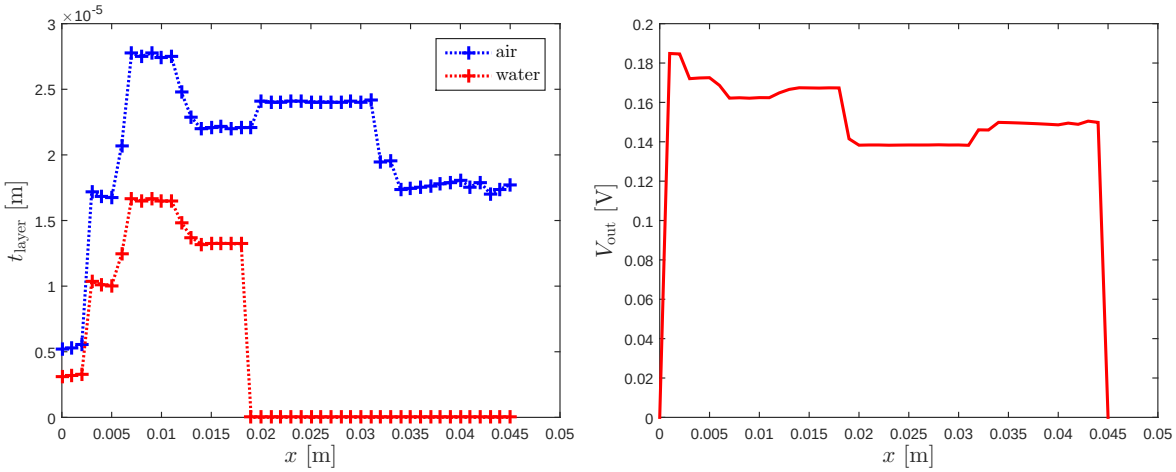

(a) *The thickness of the air layer as function of the length of the skate (here $x = 0$m is the front of the skate). The blue data represents the air thickness; the red data represents the part of the air layer filled with water. In this particular case the first 40 percent of the data points is filled for 60 percent with water.*

(b) *The predicted signal corresponding to the layer situation of figure (a). The same applies to the x-axis as mentioned in the subscript of (a). the y-axis is the expected output voltage of the system.*

Figure 4.3: *The outputs of Set-up.m: the thickness of the air layer between the skate and the ice and the matching predicted voltage peak.*

the ice and the skate could now be loaded into Set-up.m to make a more realistic prediction of the output signal. In the version of Set-up.m that was used by Van der Reep and Fennet, the program the curved skate moved over a flat piece of ice; here no virtual skate moves along: only thickness data is used to assess the predicted signal.
As mentioned in chapter 2, there may exist a water layer under the skate. For this reason the program is designed as such that a certain percentage of the air layer as produced by AirLayerSkate.m can be filled with water. The latter can be done with different percentages for four regions along the skate. For example: in figure 4.4 is the first 20 mm of the length of the skate 60 percent filled with water. The other 60 percent of the skate's length is left dry. This is just an example of how water can be filled in the program; for results see chapter 5.

4.3.3 The program *Compare_signal_characteristics.m*

To compare the processed data of multiple measurements easily the program *Compare_signal_characteristics.m* is made.
This program first loads processed data saved by the program *TTAnalysis_ziload.m*. Next the user is asked what two signals of the loaded data should be compared between measurements. These are called 'Cdata1' and 'Cdata2' Generally, the averaged data forth and back are chosen. The user is also asked if the spatial dimensions of the second group of signals (generally the back signals) have to be flipped. The results of this operation is that in the second group of signals the direction of time is reversed. The above described process aids in studying the characteristics of the structure of the ice layer and existence of a water layer. Namely by the use of symmetry: if the two

groups of signals have the same shape, than no distinction can be made in assigning a front end or rear end to the ends of the skate.

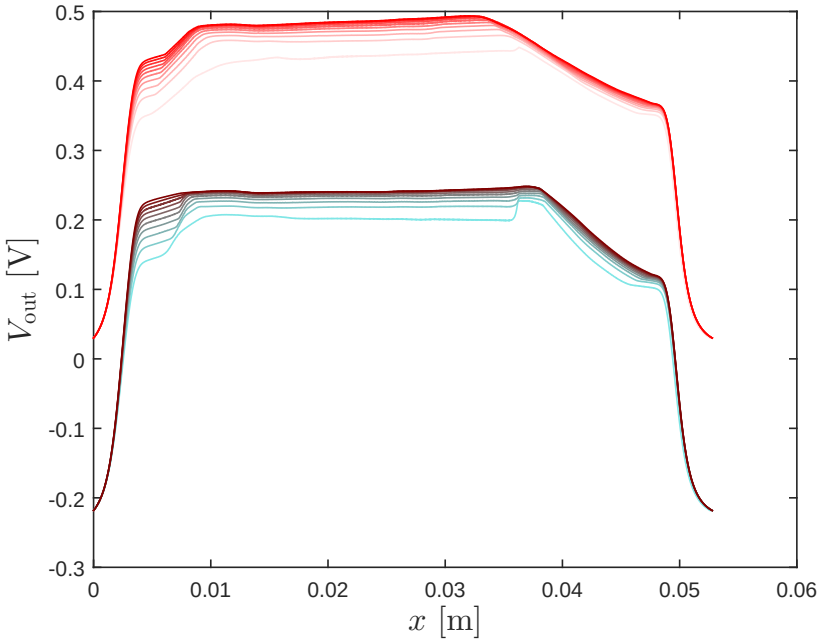

Figure 4.4: *Plot of two groups of signals in the spatial domain. The upper signals are the averaged forth signals, the lower signals (due to negative vertical translation) are the averaged back signals. The lighter red signals are earlier measurements and the darker signals are measured later. The same applies for the lower signals: blue is taken before brown.*

Next, the program made a time and a spatial axis (the length coordinate x along skate; $x = 0$ mm is the front end of the skate) for plotting. This is done using a by the user given velocity of the skate and sampling rate at witch the measurements are conducted. On this point the data of 'Cdata1' and 'Cdata2' is plotted (see figure 4.4). The group of signals designated 'Cdata1' is plotted in red. A signal with a darker color means a measurement taken later in time. As can be seen in figure 4.4, the peaks 'grow', this is due wear on the ice because of the passages of the skate.
The lower data in figure 4.4, representing the data group 'Cdata2' is translated with one half of the peak height to make the data more distictable. Here holds that brown data is more advanced in time and blue is data taken earlier.

Finally, the program found the maximum voltage of each measurement of each of the groups of signals and the according time and location along the skate for these values. These values are plotted against the measurements (see figure 4.5). This way the time evolution of the capacitance measurement can be studied in more detail.

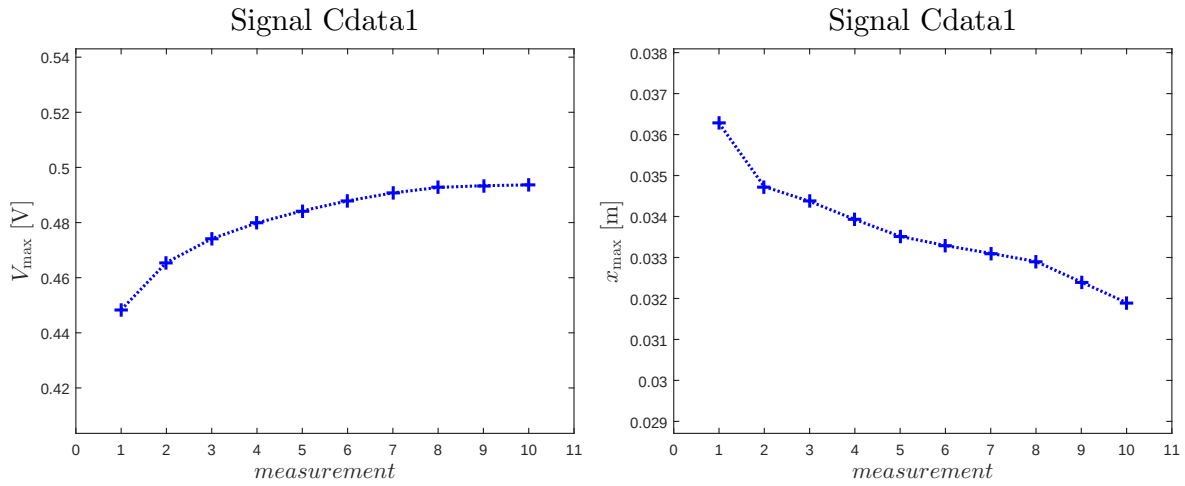

(a) *A plot of the maximum voltage as function of measurement. The maximum increases due to the skate cutting away ice and therefore getting closer to the electrode.*

(b) *A plot of the location of the maximum along the spatial axis. In this case the maximum is getting closer to the center of the skate for each measurement done.*

Figure 4.5: *Plots of the signal characteristics of the data plotted in figure 4.4 (only the forth data is shown). Every line in figure 4.4 represents one measurement on the x-axis. One measurement is an average of ten passages.*

Chapter 5

Results and discussion

This chapter will give the results obtained during the experiments conducted, as well as an interpretation of these results. The results are organized in categories each divided in results and discussion.
In section 5.1 the results of the frequency sweep data on the set-up is presented and discussed. The same is done for the noise spectrum data in section 5.2 The results of the program *Compare_signal_characteristics.m* are discussed and presented in section 5.3. The results of the gauge dial data can be found in section 5.4. Finally, the results of the program *AirLayerSkate.m* are discussed and presented in section 5.5.

5.1 Tests on the set-up: frequency sweep data

This section will cover all data obtained using the sweep function of the lock-in. The simulations are made using *Set-up.m*, see section 4.3.2. This is done to confirm the right operation of the set-up.

5.1.1 Results of frequency sweeps

In figure 5.1 a log-log plot is shown of the output voltage of the set-up against the input voltage's frequency. In all results in this section V_{in} is 1 V. In this case the skate was held in place, using the air pressure piston, directly on the kapton tape. No ice or water are present during these measurements. From 1 kHz up to 400 kHz the data fits well. After 400 kHz the fit diverges a bit around the voltage peak of 1 MHz, and after 2 MHz the prediction totally diverges from the measured values.

Next, in figure 5.2, again the output voltage as function of the frequency of the input voltage is plotted on a log-log scale. In this case a air layer is present between the skate with a thickness of 1.095 mm[1].

[1]This is measured by pressing the skate directly on a piece of metal next to the skating track and subsequently moving the skate over the electrode using the servo. The thickness is measured using calipers.

The data does not fit on any frequency, though the derivative seems to fit well. For this reason the data in figure 5.2(b) is multiplied with a factor seven. In the case in which the data is multiplied, the prediction fits the data very well up to 1 MHz, and beyond 1 MHz the prediction is close to describing the data.

Finally, in figure 5.3 the results of a sweep with a layer of ice can be observed[2]. Clearly, the data does fit even less than in the case of an air layer or absence of sample (direct contact). Only the sweep data around the peak at 2 MHz is predicted with some accuracy.

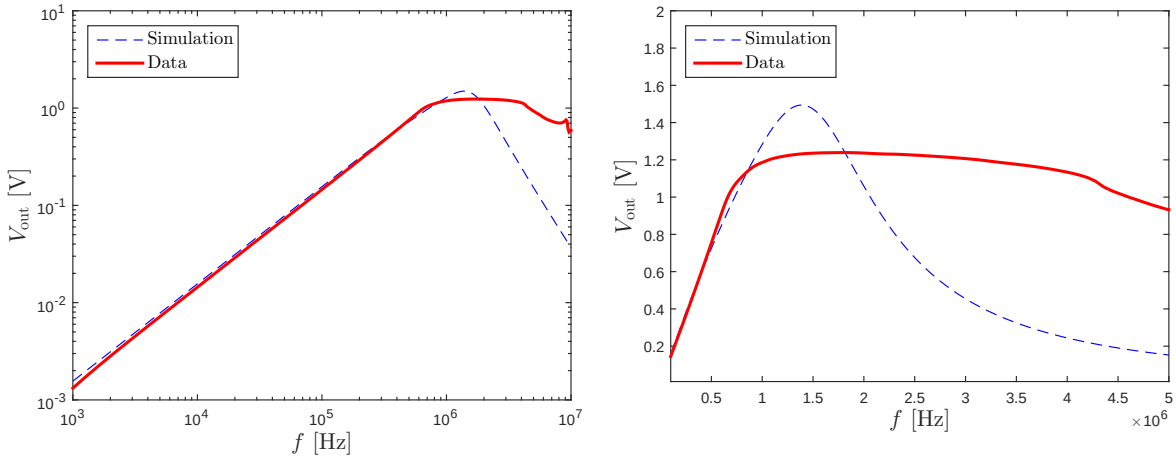

(a) *A sweep of all frequencies. Here can be seen that for the 11 kHz signal the prediction holds, for the 1 MHz signal it does not.*

(b) *A zoom of figure (a) around the 1 MHz peak. As can be clearly seen, the prediction no longer fits after 1 MHz. N.B.: this plot is on a linear scale.*

Figure 5.1: *plots of the output voltage as function of the input voltage's frequency. The skate is pressed directly to the skate-track; no water or ice are present. The red curve corresponds to measured values, the blue striped curve is the according simulation. $V_{in} = 1$ V.*

[2]During the measurement of this sweep, the dial gauge was not available. Consequently the ice thickness was estimated at 400 μm thick.

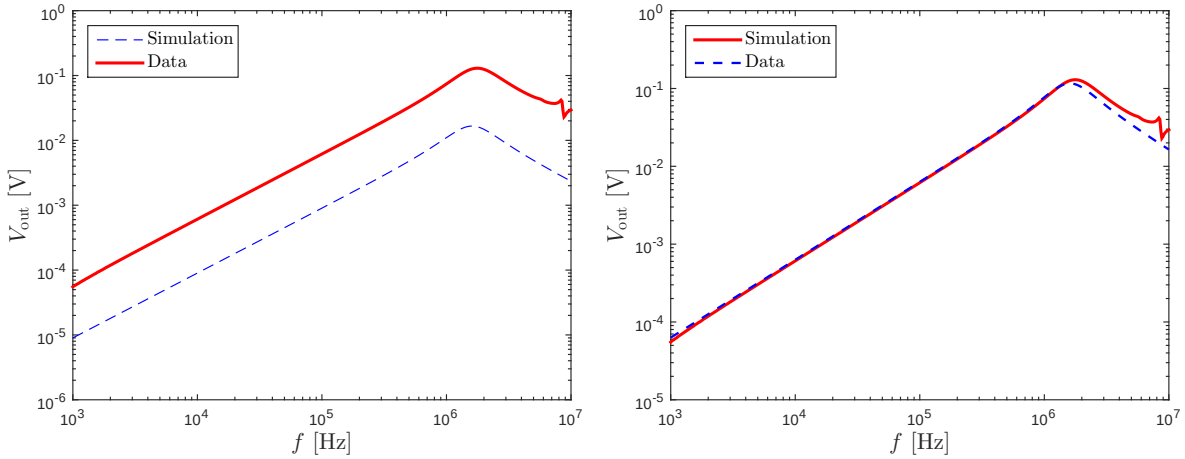

(a) *A log-log plot of the output voltage as function of the input voltage's frequency. Here can be seen that for all frequencies the prediction does not fit. Although, a constant offset is observable.*

(b) *The same data as plotted in (a). This time the prediction is multiplied with a factor 7. As can be seen, the data clearly fits in almost all frequencies. The data fits even nearly at frequencies above 1 MHz.*

Figure 5.2: *A log-log plot of the output voltage as function of the input voltage's frequency. The air layer was 1.095 mm thick. The red curve corresponds to measured values, the blue striped curve is the according simulation. $V_{in} = 1$ V.*

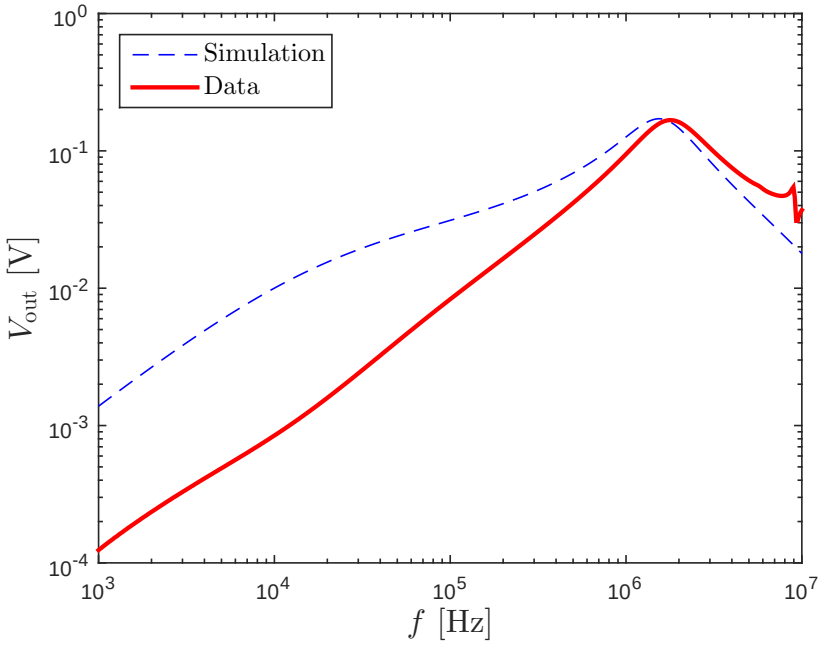

Figure 5.3: *A log-log plot of the output voltage as function of the input voltage's frequency. The sample consisted of an ice layer with a thickness of 0.4 mm (estimate, see footnote 2 of this chapter). Clearly, the data does not fit. In the measured data, as well as the predicted data, a second cut-off frequency is visible. The red curve corresponds to measured values, the blue striped curve is the according simulation. $V_{in} = 1$ V.*

5.1.2 Discussion of frequency sweeps

From the fact that the prediction of the output voltage fits the measured data in the direct contact experiment[3] (see figure 5.1(a)) we can conclude that the transfer function, as predicted in section 3.2.1, still holds after rebuilding the experiment. However the prediction does not fully cover the frequency that was used in most measurements, being the 1 MHz signal (see figure 5.1(b)).
A divergence of the prediction is expected for high frequencies, since for high f, $|q| > 1$. Moreover, the $|q|$ factor is above 1 when f is above 2 MHz, so the data to 2 MHz must fit. However it does not. From this can be concluded that the parameters in Set-up.m must be tweaked even further to ensure a better fit to reality in the case of figure 5.1.

The sweep data of the air sample fits after multiplication with a factor seven (see figure 5.2(b)), though in the direct contact measurement it does without multiplication (see figure 5.1(a)). Since the difference between the sweeps in figure 5.1 and figure 5.2 is the sample, the constant offset in the data of figure 5.2(a) originates from an unexplained effect in the sample. This could include boundary effects in the interface between kapton tape and air.
Furthermore, it can be caused by non-bulk effects due to small layer thickness. In the case of kapton, this may be true. However, in the case of an ice layer we must remember that the thickness of the premelting layer (and therefore the interface layer, where the ice structure is non-bulk) is 40,000 times smaller than the total layer thickness, since the premelting layer is predicted around the 10 nm [21], the layer thickness is approximately 400 μm thick. This means the center of the ice layer is in bulk. Form this can be concluded that unexplained effects must be modeled for a good prediction of the sweep data.

Finally, it must be noted that a second cut-off frequency is visible in the sweep data performed on the ice sample, around 10 kHz. This second cut-off is expected though the location of the cut-off is predicted at a frequency two times higher. The frequency dependence of the ice can be seen as well in the fact that the signal for high frequencies almost fits. For rightly modeling the sweep data in the case of an ice sample (figure 5.3), again a combination of tweaking the settings of *Set-up.m* for high frequencies and changing the cut-off frequencies of the dielectric constant of ice for the modeling the lower frequencies is in order. The later can be done since the cut-off frequencies of the dielectric constant of ice depent on the exact circumstances under which the ice is grown.

In Van der Reep's data $|q| > 1$ occurred at higher frequencies than in the experiments conducted here. This is not expected. This must be fixed in a later stage of the skating project.

A parameter that needs tweaking is the paracitic capacitance, since all frequency sweeps are not fitted above 1 MHz. The cut-off in the high frequency range is determained by the paracitic capacitance. So if tweaked correctly, a fit to 2 MHz can be achieved.

[3] Tom van der Reep calls this 'the simplest experiment'.

5.2 Tests on the set-up: noise data

This section will cover the measured noise spectrum of the set-up for low and high frequencies. Predictions made by Set-up.m are evaluated as well.

5.2.1 Results of noise spectrum

In figure 5.4 the results of the measurement of the noise spectrum are plotted. These spectra are taken with the servo and the thermoelectric cooler turned off.

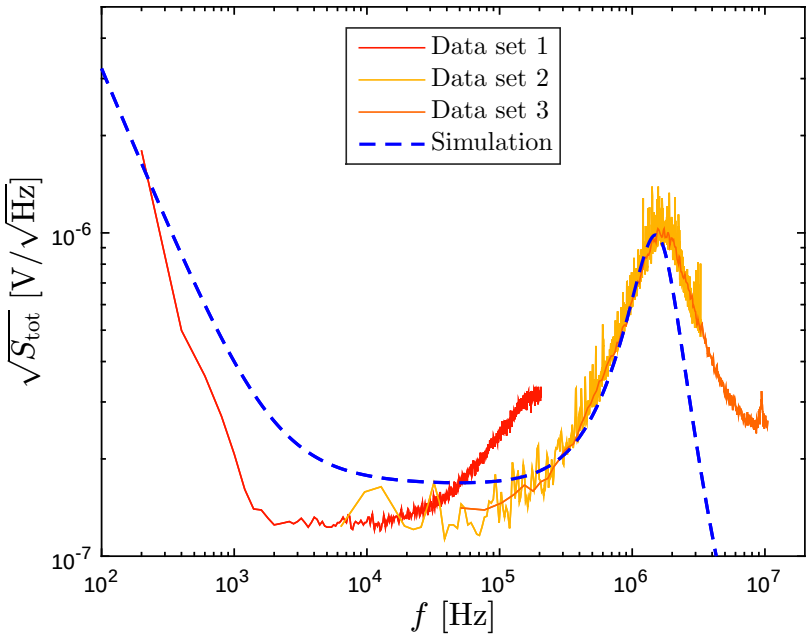

Figure 5.4: *plots of the noise spectrum together with a plot of the prediction of the noise spectrum using Set-up.m. The red and orange curves are measured data sets in their applicable frequency range, the blue striped curve is the according simulation.*

5.2.2 Discussion of noise spectrum

As can be seen in figure 5.4 does the simulation fit the data very well up to about 2 MHz. From this point on, it is expected that $|q| > 1$. This means that the theory does not hold any more form this point and no fit is expected (see section 3.2.1). The large peak around 2 MHz is due to the noise coming from the IV-converter's opamp.

The noise spectrum of the low frequencies in figure 5.4 is simulated with less precision. The bump in data set arount 200 kHz is caused by binning effects, as can be deducted from the fact that the data around these frequencies does fit the other two (in this region applicable) data sets. The prediction of the noise at frequencies lower than 50 kHz is higher than measured, which is quite convenient, because the noise on the 11 kHz measurements have a factor 2 less noise than predicted. The large increase of noise in the lower frequency range is due to 1/f-noise caused by the lock-in amplifier.

5.3 Comparing signal characteristics

The results of the use of the program *Compare_signal_characteristics.m* are evaluated in this section. These consist of plots of the averaged data peaks, as well as evaluations of the location and magnitude maximum in these peaks.

5.3.1 Results of the usage of *Compare_signal_characteristics.m*

In figure 5.5 averaged voltage peaks can be observed as function of the length coordinate along the skate. $x = 0$ m corresponds to the front end of the skate. As discussed in section 4.3.3, the lower sets of data are translated by half a peak height and the dimensions of the lower sets of data are flipped[4]. The data is averaged over ten passages, so each curve in figure 5.5 represents ten passages. The data is acquired on electrode 11 and on the new ice track. As can clearly be seen the data contains 'shoulders' and does the maximum voltage increase each ten passes. The 'shoulders' are sudden in- or decreases in voltage near the end of the skate. A lighter color of the curve corresponds to a measurement earlier.

Figure 5.6 shows a typical result from the old skating track. These results are taken on electrode 10. The same operations are conducted as on the data depicted in figure 5.5. The data is analyzed for the maximum voltage of each curve, as well as the location along the skate's length where this maximum occurred. For the results see figure 5.7 and figure 5.8.

The general findings are now presented. 'Shoulders' are a common feature on the data, though not all voltage peaks possess them. Most of the measurements conducted on the new track have larger 'shoulders' on the right than on the left.
Most measurements, especially the ones conducted after the skate has passed multiple times, tend to be symmetric in the spatial domain. This symmetry is only general, since in most cases in the right 'shoulder' of the back peaks in the measurements taken earlier the voltage is higher than in the measurements taken later. This was the other way around for the forth peaks.
On the new skate-track the variations in the x-coordinate of the maximum voltage are less big than the variations of this coordinate during measurements taken on the old track.

[4]This means times runs backwards in the downward translated data.

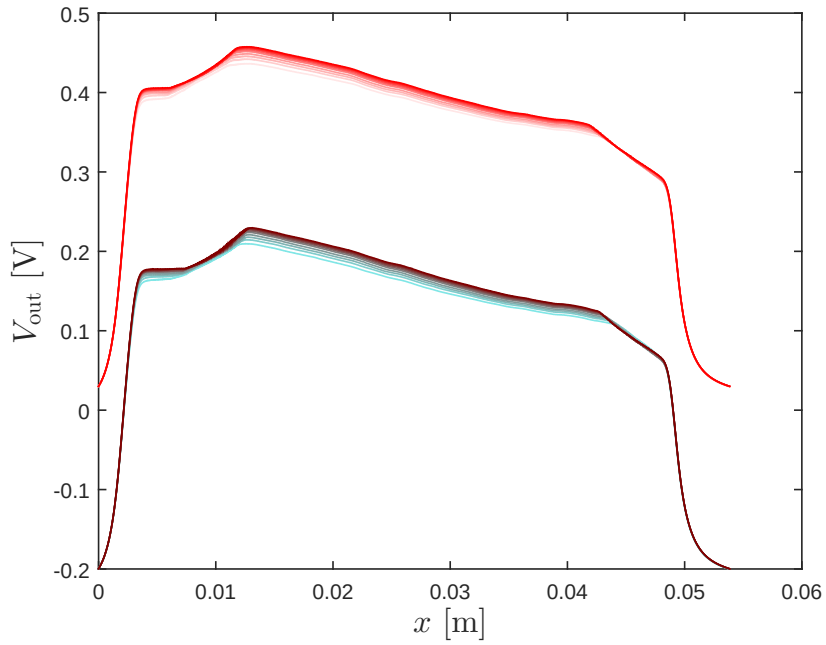

Figure 5.5: *A plot of the output voltage of the averaged signal as function of the skate's length (here $x = 0$ m is the front of the skate if the skate is moving forth). The upper data is taken when the skate moved forth, the lower data when the skate moved back. The lower data is translated with half a peaks height. $v_{skate} = 50$ mm/s, $p = 0.3$ bar, experiment conducted at electrode 11. Note the 'shoulders': around $x = 5$ mm and around $x = 46$ mm. Data obtained on the new track.*

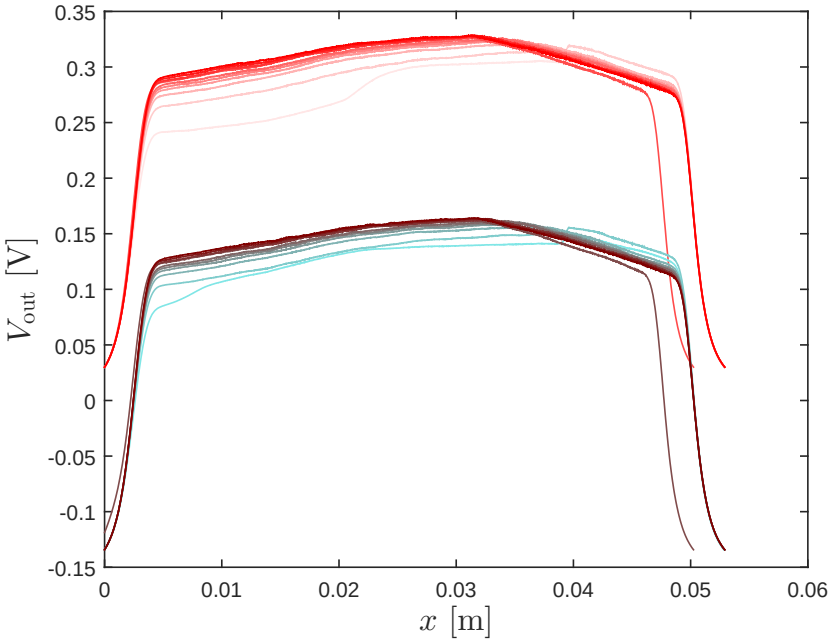

Figure 5.6: *A plot of the output voltage of the averaged signal as function of the skate's length (here $x = 0$ m is the front of the skate if the skate is moving forth). The upper data is taken when the skate moved forth, the lower data when the skate moved back. The lower data is translated with half a peaks height. $v_{skate} = 25$ mm/s, $p = 0.3$ bar, experiment conducted at electrode 10. Note that the 'shoulders' are absent. Data obtained on the old track.*

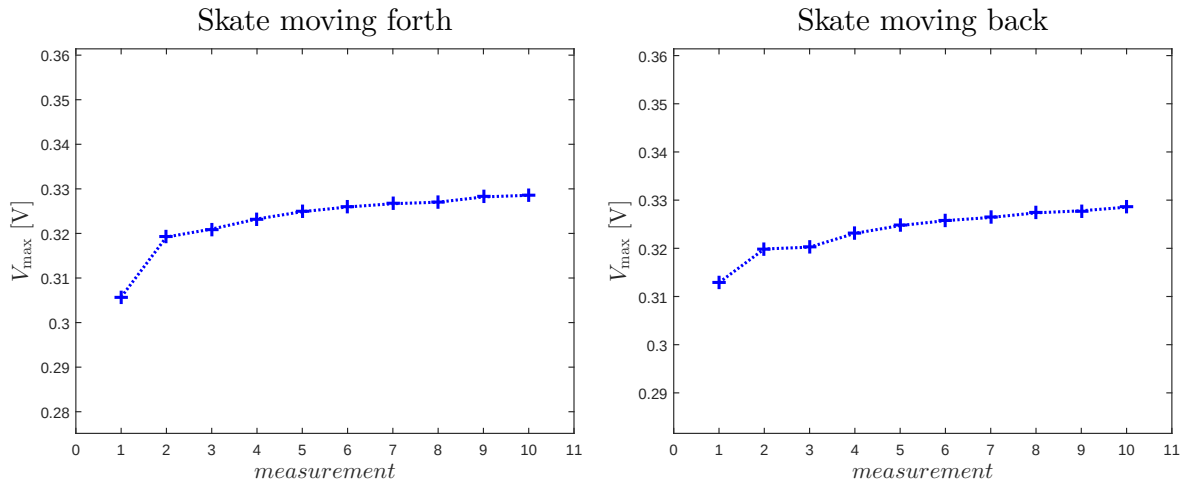

(a) *The maximum voltage of the first (higher; forth) set of signals in figure 5.6 as function of the measurement conducted (each average of ten times forth and back).*

(b) *The maximum voltage of the second (lower; back) set of signals in figure 5.6 as function of the measurement conducted (each average of ten times forth and back).*

Figure 5.7: *Plots of the maximum voltage as function of the measurement done. Clearly the maximum voltage does increase strongly in the first measurements, and less strongly in the later measurements.*

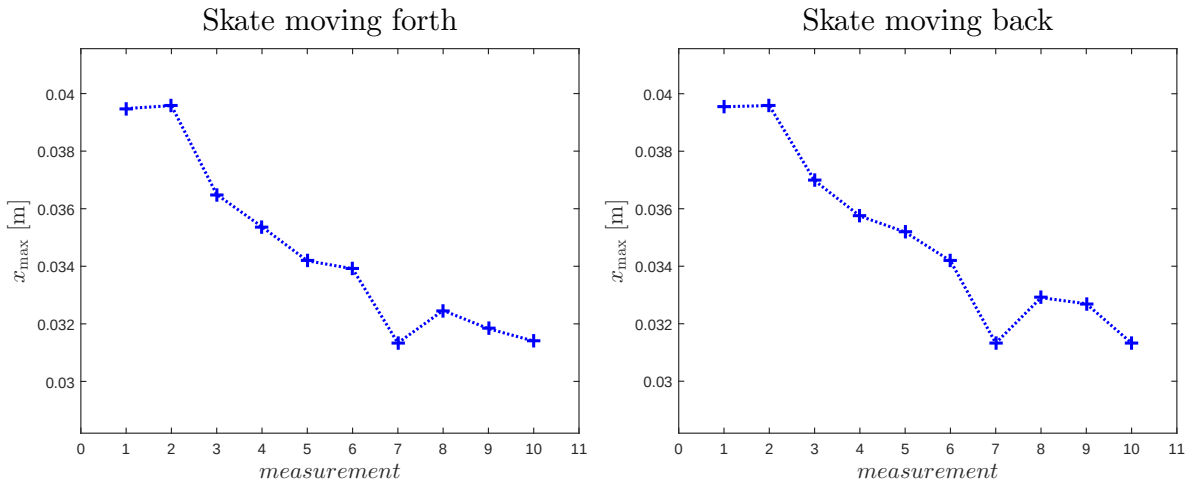

(a) *The location along the skate's length where the maximum voltage of the first (higher; forth) set of signals in figure 5.6 is found.*

(b) *The location along the skate's length where the maximum voltage of the second (lower; back) set of signals in figure 5.6 is found.*

Figure 5.8: *Plots of the location along the skate where the maximum voltage is found, as function of the measurement done. The location of the maximum varied in this case quite heavily, from 40 mm from the front of the skate to 30 mm from the front of the skate.*

5.3.2 Discussion of the usage of *Compare_signal_characteristics.m*

Remarkable of the data shown in figure 5.7 is that the maximum voltage typically increases quite strongly in the first measurements and less strongly in the later measurements. This means that the skate gets closer to the electrode after each measurement. implicated is that the top of the ice layer disappears in all the measurements. This could be due for example to melting by frictional heating or due to the skate scraping ice away.
If the ice disappears under the skate, a track could be formed. This track could be formed in such a way that the skate makes contact with the ice on the sides of the skate. This may cause that the ice melts less quick in later measurements.
it is also possible that the disappearance of the top layer of ice causes the skate to have a bigger contact area on the ice. This means more ice can be melted or scraped away in later measurements. This explains that in later measurements the maximum voltage increases less than during measurements completed earlier in time.

For both signals forth and back the location at which the maximums occur shifts, in the case of the typical signal of figure 5.6. This is possibly due to the disappearance of bumps in the ice surface and might tell us something about the structure of the ice layer. This can be explained the following way. If an bump in the ice exists, the skate and the ice will, at locations around this bump, not be in contact. This creates a cavity between the ice and the skate which is filled with a combination of air, water and ice shavings. If a certain cavity exists above an electrode, the signal will be influenced: the maximum signal can not be in the center of the skate[5]. If the bump disappears, the shape and possibly the medium of this cavity will change; the ice layer will become more and more flat. If the maximum voltage in earlier measurements occurs on the rear side of the skate (if the skate moved forth, so $x_{\max} > 2.5$ cm), then a bump in the ice exists at the left side of the electrode which disappears. If the maximum voltage in earlier measurements occurs on the front side of the skate (if the skate moved forth, so $x_{\max} < 2.5$ cm), then a bump in the ice exists at the right side of the electrode which disappears. So in the case of figure 5.8 there was a bump on the left side of the electrode.

This does not explain the the 'shoulders' in the data that can be observed in figure 5.5, since these are absent in figure 5.6. For a further discussion of the 'shoulders' see section 5.5.

The general symetric behavior of the voltage peaks in the spatial domain suggests that the shape of the skate is symmetric, as well as the way the skate slides over the ice. To put this in other words: if the skate reverses and the backside of the skate becomes the front side of the skate, than so does the behavior.
The broken symmetry as explained in the results section could be due to the fact that the skate can rotate freely in the vertical plane aligned with the direction of motion. When the skate reverses direction, the skate will rotate, so the front end gets lower than the rear end.

[5]This is expected in a the case of a totally flat ice layer.

If the skate, in later measurements, experiences more friction due to a larger contact area[6], this rotation is quicker and the signal is higher. This explains why in later measurements the output voltage in the right 'shoulders' of the back peaks is lower than in measurements conducted earlier. More measurements using the new force sensor must be done to verify this hypothesis.

From the fact that the variations in the x-coordinate of the maximum voltage are less big than the variations on the old track, we can conclude that either the ice disappears more quick on the bumps on the old track than the new track or the bumps in the ice are less thick on the new track. Since there are no reasons to expect the first (see section 5.4), the later hypothesis is more favoured.

5.4 Dial gauge data

This section covers the data obtained using the dial gauge as discussed in section 3.4.

5.4.1 Results of the dial gauge data

Figures 5.9 to 5.13 represent dial gauge data taken on the old skate track. In figure 5.9 the definition $(x_{\text{dial gauge}}, d_{\text{ice}}) = (0, 0)$ is made visible. What becomes directly apparent is that, what was expected in the discussion of the data processed by the program *Compare_signal_characteristics.m*, is confirmed. The ice is not a flat structure. Furthermore, the variations in ice thickness are a up to a factor 20 bigger than the height variations of the skate[7] due to the curvature of the skate.
Other findings obtained on the old skate-track include a bump in the ice which is present, on different ice layers with different thicknesses, on the same location. This bump has a maximum at $x_{\text{dial gauge}} = 94$ mm to $x_{\text{dial gauge}} = 97$ mm. This bump is always followed by a dip in ice thickness around $x_{\text{dial gauge}} = 105$ mm (see figures 5.9 and 5.10). After this a rough patch is observed with a lot of variation in the ice thickness (see figure 5.13). This rough patch is extended between $x_{\text{dial gauge}} = 115$ mm and $x_{\text{dial gauge}} = 150$ mm.

An especially nice example of the bump is visible in figure 5.10. In this case the bump is 100 μm lower after skating a hundred times forth and a hundred times back. Moreover, the bump is more flat after skating than before. In figure 5.11 the voltage peaks are plotted using the program
Compare_signal_characteristics.m. These peaks are obtained using electrode 10, which is situated next to the bump. Striking is that the location of maximum voltage along the length of the skate is strongly decreasing. In the earlier measurements the maximum voltage was found almost 40 mm from the beginning of the skate. In the last measurement this is 22 mm from the front end, as can be seen in figure 5.12(b). Figure 5.12(a) shows the magnitude of the maximum voltage of the peaks in figure 5.11.

[6]The skate has made a track and is in contact with the ice on the sides. See the discussion of figure 5.7. This needs verification as well, by using the dial gauge to develop insights in the track witch is formed by skating.

[7]Remember: the sides of the skate are approximately 10 μm higher than the middle of the skate.

On the new skate track the constant bumps are not visible anymore. The ice thickness varies between different ice layers. Sometimes the ice layer is ascending along $x_{\text{dial gauge}}$ (see figure 5.14), sometimes descending (see figure 5.17). Generally, the height variations in the ice layer thickness are less big when the ice is grown on the new skate-track[8].
When the height variations are significantly less (only a factor 5 in comparison to the height variations of the skate) the voltage peaks became completely symmetric in the spatial domain, as can be seen in figure 5.15. The location of the maximum along the length of the skate is in this case almost constant (see figure 5.16(b)). Besides, the increase in the maximum seems to have become linear in this case, as depicted in figure 5.16(a). However, the first measurement (average over ten passages) is missing, due to incautious handling of the data.

The measurements conducted on the new ice-track have brought a drawback of the dial gauge to the surface. Sometimes the measurements conducted after the skating give a thicker ice layer, than before skating (see figure 5.17). However, the height profile remains mostly the same.

In all figures presented in this section, the vertical blue line represents the location of electrode 10 under the ice.

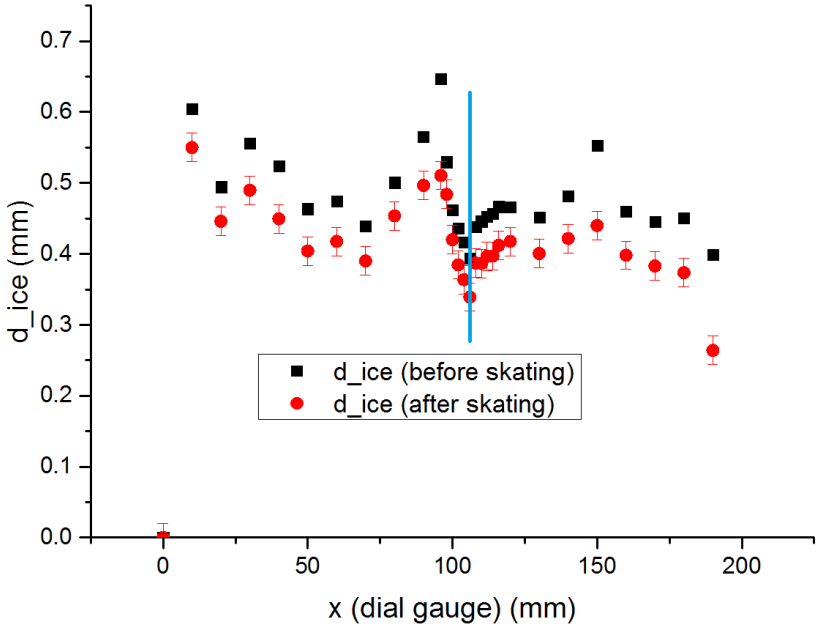

Figure 5.9: *A plot of the ice thickness as function of the location of the dial gauge. This data is obtained on the old skate-track. The black data is obtained before skating; the red data after. The vertical blue line indicates the location of the electrode under the ice. The error bars in the black data are to small to be visible (± 5 μm; see section 4.1). The bump around $x_{dial\ gauge} = 95$ mm is visible just before the electrode. The dip is visible around the electrode. The definition of $(x_{dial\ gauge}, d_{ice}) = (0, 0)$ is made visible.*

[8]N.B.: Since the thickness of the surface of the new ice track could not be evaluated without damaging the skate track (see section 3.3), the y-axis, in the figures displaying data obtained on the new skate-track, are labeled h_ice, not d_ice. This means the values are not corrected, and are the raw data points. The data labeled with d_ice on the y-axis is corrected as described in footnote 1 of chapter 4.

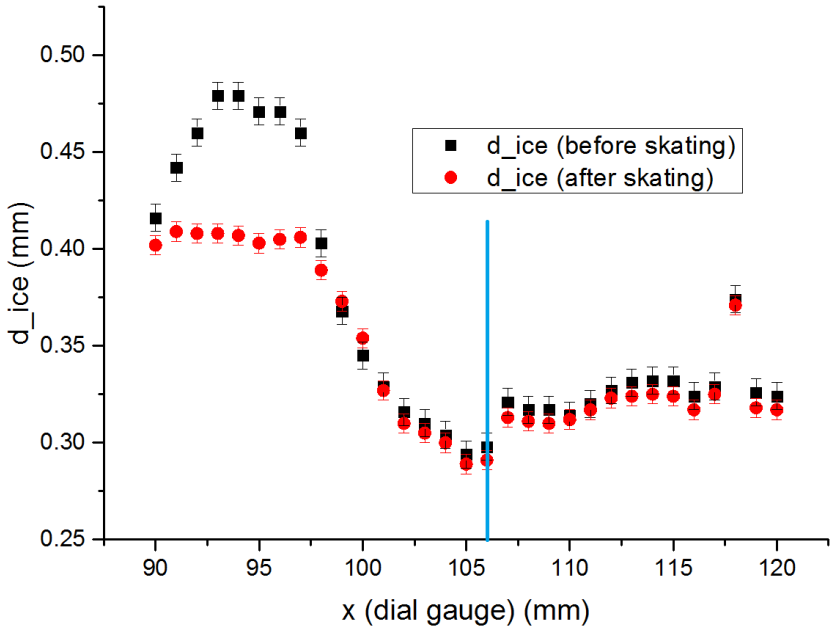

Figure 5.10: *A plot of the ice thickness as function of the location of the dial gauge. This data is obtained on the old skate-track. The black data is obtained before skating; the red data after. The vertical blue line indicates the location of the electrode under the ice. The bump around $x_{dial\ gauge} = 95$ mm is visible just before the electrode. After skating the bump is lowered and flattened.*

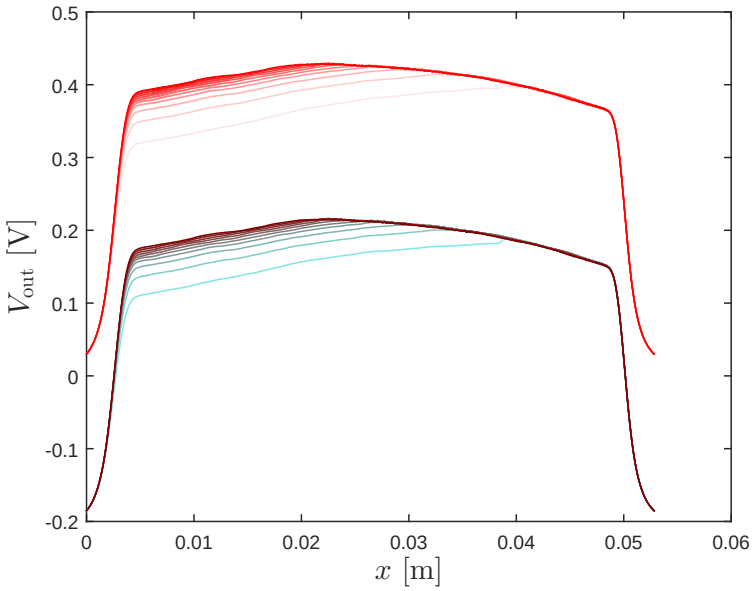

Figure 5.11: *The voltage peaks obtained on the ice layer plotted in figure 5.10. The output voltage is plotted as function of the skate's length (here $x = 0$m is the front of the skate if the skate moved forth). The upper data is obtained with the skated moving forward; the lower data with the skate moving back. The lower data was translated with half a peak's height. $v_{skate} = 100$ mm/s, $p = 0.3$ bar, experiment conducted at electrode 10. Note the shift of the maximum from the rear of the skate to the front.*

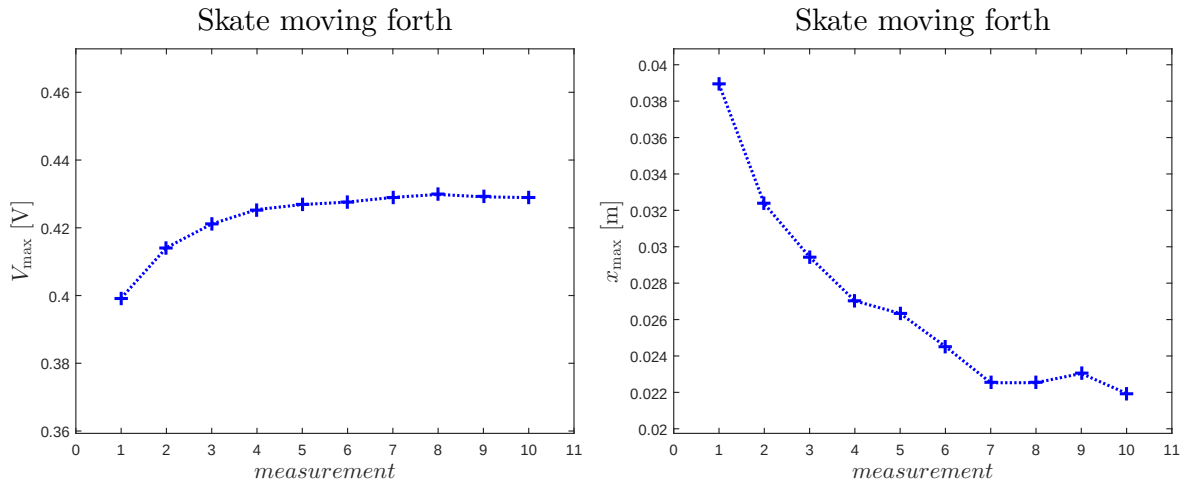

(a) *A plot of the magnitude of the maximum voltage as function of the measurement conducted. In the earlier measurements the maximum voltage increased faster than during later measurements.*

(b) *A plot of the location of the maximum voltage along the skate's length. Striking is the huge difference between the first measurement and the last measurement: in the first measurement the maximum is around the rear of the skate ($x_{max} = 40$ mm), in the last the maximum is around the beginning of the skate ($x_{max} = 22$ mm).*

Figure 5.12: *Plots of the magnitude (a) and the location (b) of the maximum voltage of the voltage peaks in figure 5.11.*

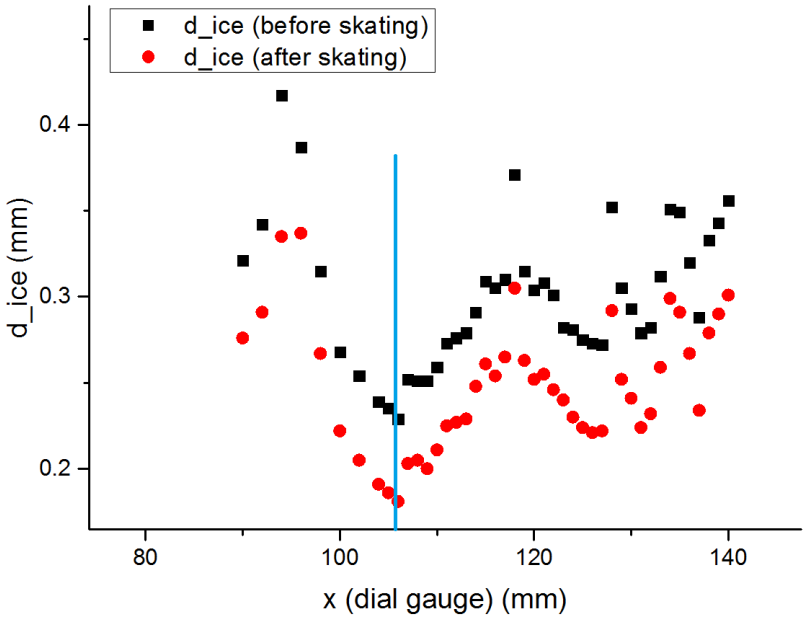

Figure 5.13: *A plot of the ice thickness as function of the location of the dial gauge. This data is obtained on the old skate-track. The black data is obtained before skating; the red data after. The vertical blue line indicates the location of the electrode under the ice. The error bars in the data are to small to be visible (± 5 μm). The bump around $x_{dial\ gauge} = 95$ mm is again visible just before the electrode. The dip is visible around the electrode. After $x_{dial\ gauge} = 115$ mm the rough patch is visible.*

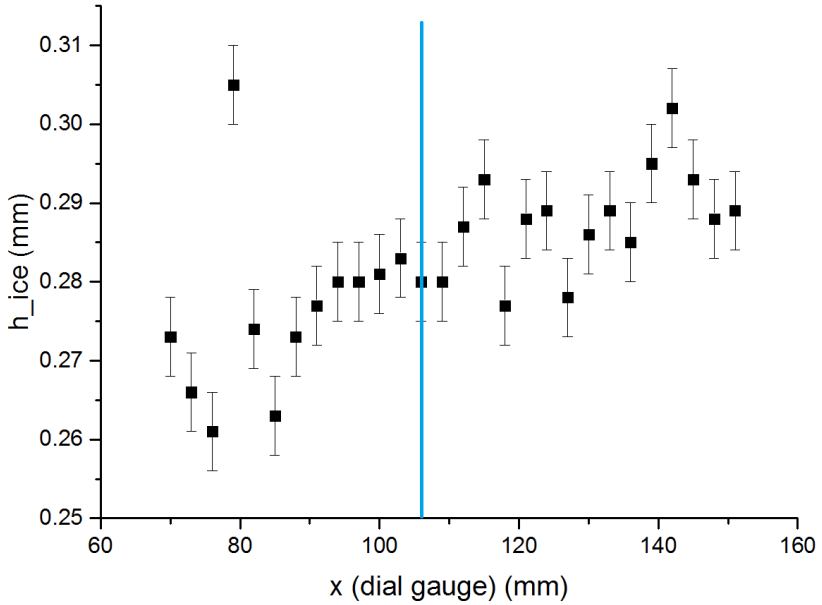

Figure 5.14: *A plot of the ice thickness as function of the location of the dial gauge. This data is obtained on the new skate-track. The data is obtained before skating. The vertical blue line indicates the location of the electrode under the ice. Since this data is obtained on the new skate-track, the height variations are much reduced with respect to the old skate-track.*

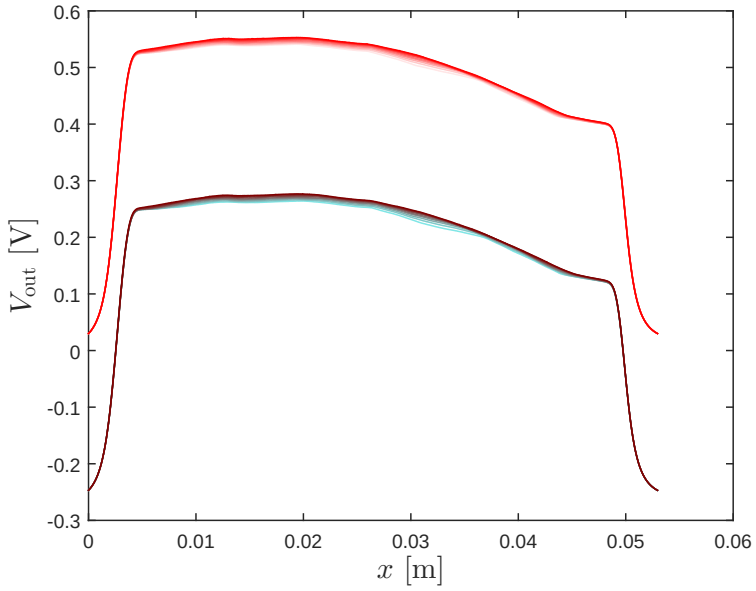

Figure 5.15: *The voltage peaks obtained on the ice layer plotted in figure 5.14. The output voltage is plotted as function of the skate's length (here $x = 0$ m is the front of the skate). The upper data is obtained with the skated moving forward; the lower data with the skate moving back. The lower data is translated with half a peak's height. $v_{skate} = 50$ mm/s, $p = 0.3$ bar, experiment conducted at electrode 10. Note that the peaks are completely symmetric in the spatial domain and remain fairly constant.*

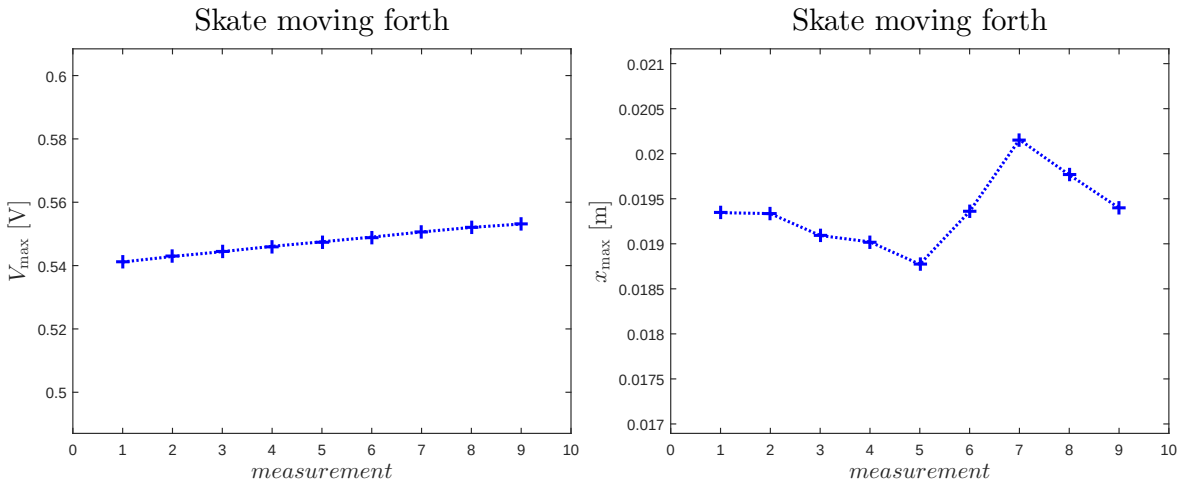

(a) *A plot of the magnitude of the maximum voltage as function of the measurement conducted. The voltage increase is completely constant. However, the first measurement is missing (here depicted as missing the tenth measurement).*

(b) *A plot of the location of the maximum voltage along the skate's length. The location of the maximum voltage remains more or less constant during these measurements.*

Figure 5.16: *Plots of the magnitude (a) and the location (b) of the maximum voltage of the voltage peaks in figure 5.15.*

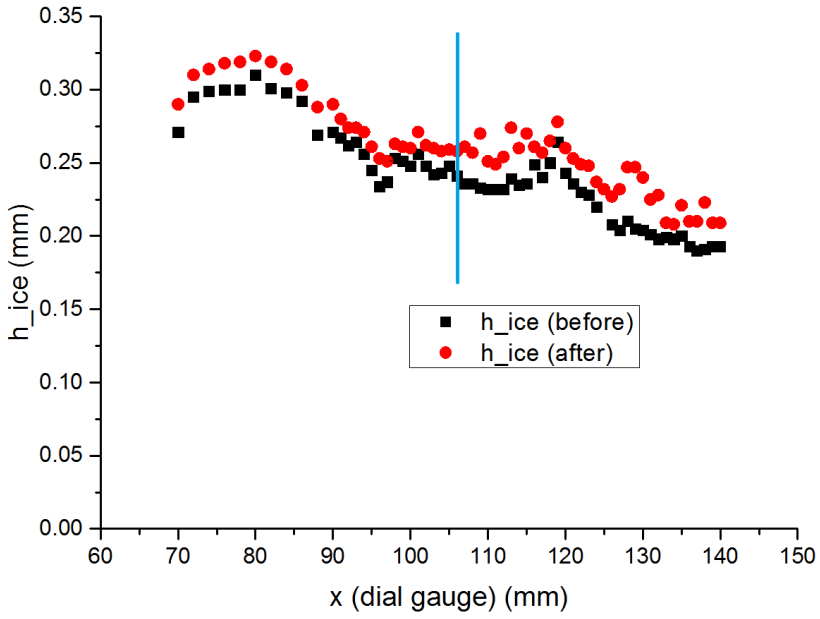

Figure 5.17: *A plot of the ice thickness as function of the location of the dial gauge. This data is obtained on the new skate-track. The black data is obtained before skating; the red data after. The vertical blue line indicates the location of the electrode under the ice. The error bars in the black data are to small to be visible (± 5 μm). This indicates that the variation in the thickness of the ice layer has become less on the new track. Note that the after skating measurements are higher than the before skating measurements, though the general height profile is the same.*

5.4.2 Discussion of the dial gauge data

A remarkable feature of the data is the reoccurring bump, as well as the reoccurring dip and rough patch, when ice is grown on the old skate track. This may be caused by the the way the tape is aligned on the sides of the skate track. The surface of the skate track (kapton tape) is hydrophobic. This means the water is 'hung up' on the layers of tape on the sides of the track. Therefore, if the skate-track is slightly wider, the ice layer will be slightly thicker. This could explain why the certain features of the ice layer were present in different layers of ice.

In figure 5.10 the bump in the ice is very clear. This confirms the thoughts about a cavity in which a combination of media reside, as formulated in section 5.3.2. After skating the bump seems to be 'skated of'. The process by which the bump disappears, can not be specified at this point. Options are frictional heating or scraping of parts of the ice due to passage the skate. The disappearing of the bump is supported by the data in figures 5.11 and 5.12. As discussed in section 5.3.2, a large shift in the maximum voltage due to a bump ice is observable. In section 5.3.2 a bump on the left side of the electrode is predicted, this is confirmed by the dial gauge data.
A hypothesis for the explanation of the curve of figure 5.12(a) can be formed. The bump has a wider section further down in the ice layer than on the top of the bump (as mentioned in section 5.3.2). The contact area of the skate and the ice layer increases if the bump is 'skated of' by the passage of the skate. In every measurement in this case more ice has to be removed than in the measurement before. This limits the amount of ice that can be removed per passage, yielding a curve like the one in figure 5.12(a). Further investigation has to be done to exclude hypotheses and come to a final theory (see chapter 6).

The ice grown on the new skate-track does not exhibit the same intrinsic characteristics as ice grown on the old track. Since, the surface of the new skate-track is no longer hydrophobic, the way the water layer was formed no longer depends on the layers of tape on the sides of the track. The remaining effects of the sides of the track are reduced by broadening the track. What might dominate the formation of the height profile of the ice layer on the new track, are the viscoelastic properties of water[9].

The linear behavior of the curve in figure 5.16(a) could be explained by relative a flat layer of ice, as displayed in figure 5.14. This can not be confirmed however, because the data of the first measurement is missing. N.B.: the symmetry of the forth and back peaks, together with the data in figure 5.16(b), do support the hypothesis that the ice does not contain bumps.

The drawback of the gauge dial as formulated in the previous section is a minor one. since the thickness of the ice is reported being bigger after skating than before, no serious claims can be made about the absolute value of the ice layer thickness. However, since the height profile of the ice layer remained globally the same, relative differences (i.e. bumps) can be studied. Besides, the results of the program AirLayerSkate.m are solely based on relative differences, and therefore applicable.

[9]This is based on the experience of the author: while applying water on the track, the capillary forces of the pipette could be used to transport water from one side of the track to another.

5.5 Results using *AirLayerSkate.m*

The results of the previous sections will be combined in the use of the program *AirLayerSkate.m*. The results of this program will be presented in this section.

5.5.1 Results of the usage of *AirLayerSkate.m*

Figure 5.19(a) shows a plot of the average output voltage of the forth passages 90 to 100[10] combined with the prediction derived using the data of AirlayerSkate.m. The simulation is based on a situation where the cavity between the skate and the ice is not filled with water and just with air, as can be seen in figure 5.19(b). Figure 5.19(b) is a plot of the composition of the cavity as function of the skate's length in this case. During the simulation the ice layer thickness was set to 0 μm. the fact that the magnitude of the output voltage matches to some extend is purely coincidental.
As can be seen in figure 5.19(a) the prediction does not fit the measurement of the actual output voltage. However, certain features seem to overlap. The measured data has a kink around 33 mm of the skate's length. The prediction clearly has, at the same location, some sort of kink as well. The same seems to be true at $x = 8$ mm.
Because the signal studied is a measurement of the passages 90 to 100[11], the after skating dial gauge data is used for AirlayerSkate.m. The raw dial gauge data is shown in figure 5.18 together with a screen shot of the program AirLayerSkate.m.

In figure 5.20 both graphs depict the same measurements as in figure 5.19. In this simulation however, the cavity between the skate and the ice is partially filled with water. In table 5.1 it is shown how the water is distributed over the cavity. This is again depicted in figure 5.20(b). To correct for the magnitude of the prediction of the signal, the prediction is multiplied with a factor 0.46. In this simulation no ice layer is present. These results only cover the shape of the voltage peak
The shape of the prediction fits the data better in this case than in the case with no water present.

Next, in figure 5.21(a), The process is repeated with the same measurement. This time a layer of ice is added in the simulations, with a thickness as measured by the dial gauge[12]. The way the water is distributed is changed with respect to the simulation without ice. The new values are presented in table 5.2 and figure 5.21(b). The prediction of the data is multiplied with a factor 3.2 to take care of the offset discussed in section 5.1.2.
The data seems to fit even better. Less water is required to make the data fit and water was only simulated around the center.

In figure 5.22, the process is repeated for the final time. In this simulation the cavity only contains water, as can be seen in figure 5.22(b). The prediction is multiplied with a factor 2.8 for the reasons mentioned above. The data does not fit at all and the characteristic kinks are nowhere to be found.

[10] This corresponds to measurement 10 in figure 4.4.
[11] These were the last measurements taken on this measurement run.
[12] $h_{\text{ice}} = 318$ μm.

Now a data set containing no 'shoulders' will be presented. The used data is the first ten averages, while the skate moved forth, of the data presented in figure 5.15, which are obtained on a relatively flat ice layer. Figure 5.23(a) is a plot of this data together with a simulation as discussed above. Figure 5.23(b) is a plot of the layer thickness in the cavity, as discussed above. During the simulation an ice layer is present with a thickness $h_{\text{ice}} = 280\ \mu$m. The data is multiplied with a factor 2.8.
Though the shape of the prediction does not fit the overall shape of the measured data, the general descent of the voltage signal is predicted correctly. Furthermore, the 'shoulders' are absent like in the data.

Finally, in figure 5.24(a) the simulation is repeated for the last time. The same data as in figure 5.23 is used. This simulation, in contrast to the previous simulation, the cavity was partially filled with water (see table 5.3 and figure 5.24(b)). Again the prediction was multiplied with a factor 2.8.
The data fits better than in the case of the cavity being solely filled with air. The simulation data still contains no 'shoulders'.

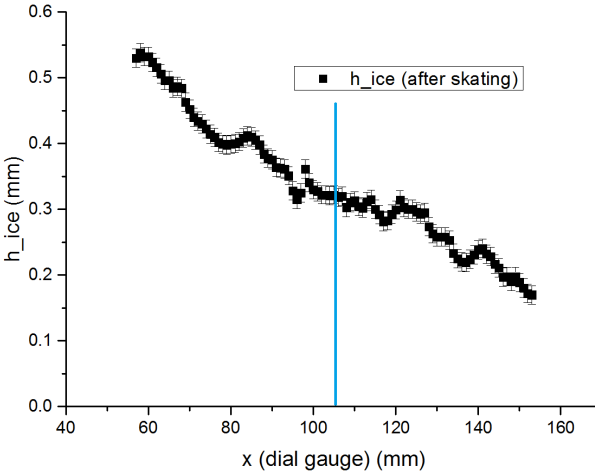

(a) *The dial gauge data that was used in making the predictions of figures 5.19 to 5.22. The black data is the thickness of the ice layer as function of the location of the dial gauge. The data is obtained after skating. The blue line indicates the location of the electrode under the ice layer.*

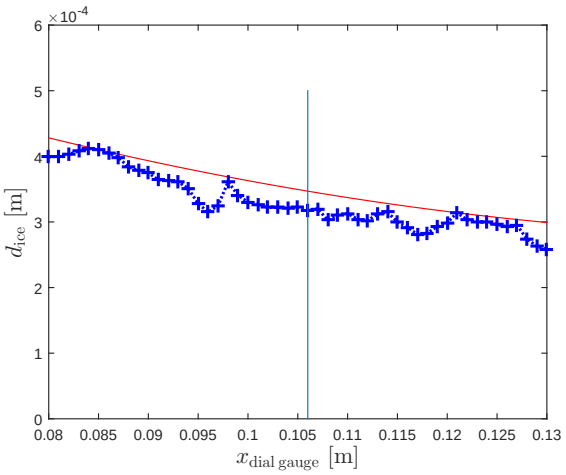

(b) *The dial gauge data from figure (a) used in AirLayerSkate.m. The skate is lowered upon the ice and at the vertical blue line (location of the electrode) the height of the cavity can be observed.*

Figure 5.18: *The dial gauge data that is used in making the predictions of figures 5.19 to 5.22, presented as raw data (a) and as used data in AirLayerSkate.m (b).*

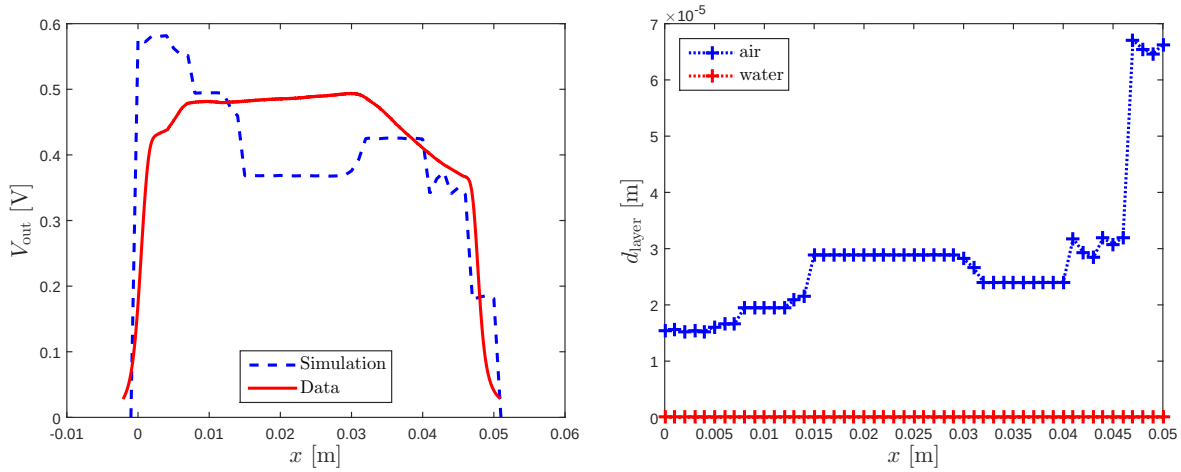

(a) *Plot of the output voltage as function of the skate's length together with the according prediction. In this simulation no ice layer was present. The general shape of the prediction does not match the data. However at the location of the top sides of the 'shoulders' in the data, the predictions seems to make kinks.*

(b) *Plot of the composition of the cavity between the skate and the ice layer. In this case this cavity is entirely filled with air.*

Figure 5.19: *Simulation of a measurement consisting of the output voltage of the system averaged over ten forth passages (being passages 90 to 100). $v_{skate} = 50$ mm/s, $p = 1.5$ bar, experiment conducted at electrode 10. In this simulation no water and no ice are present.*

Table 5.1: *The way the water is distributed over the cavity between the skate and the ice. In the first column the part of the skate's length which is filled with water, is shown. The second column depicts the percentage of the cavity is filled with water: if this percentage is 50 the other half is filled with air. These values are used in making the simulation of figure 5.20.*

Part of the skate's length (x)	**Percentage of cavity's height filled with water**
From 0 mm to 10 mm	60% water
From 10 mm to 33 mm	87% water
From 33 mm to 44 mm	80% water
From 44 mm to 50 mm	60% water

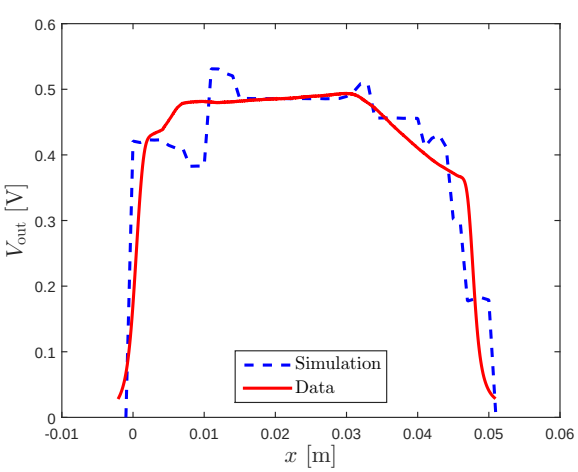

(a) *Plot of the output voltage as function of the skate's length together with the according prediction. In this simulation no ice layer was present. The prediction is multiplied with a factor 0.46 to correct for the magnitude of the signal. The prediction fits the data beter than in the case without water in the cavity. Note that the prediction has 'shoulders'.*

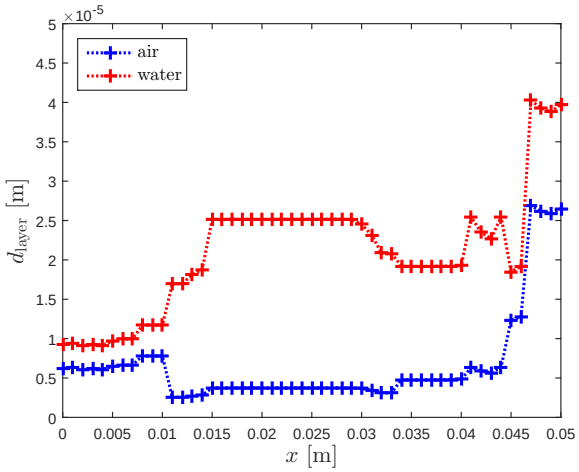

(b) *Plot of the composition of the cavity between the skate and the ice layer. In this simulation this cavity is partially filled with air, partially filled with water.*

Figure 5.20: *Simulation of a measurement consisting of the output voltage of the system averaged over ten forth passages (being passages 90 to 100). $v_{skate} = 50$ mm/s, $p = 1.5$ bar, experiment conducted at electrode 10. In this simulation water is present; ice is not.*

Table 5.2: *The way the water is distributed over the cavity between the skate and the ice. The columns have the same meaning in table 5.1. These values are used in making the simulation of figure 5.21.*

Part of the skate's length (x)	**Percentage of cavity's height filled with water**
From 0 mm to 10 mm	0% water
From 10 mm to 33 mm	70% water
From 33 mm to 40 mm	50% water
From 40 mm to 50 mm	0% water

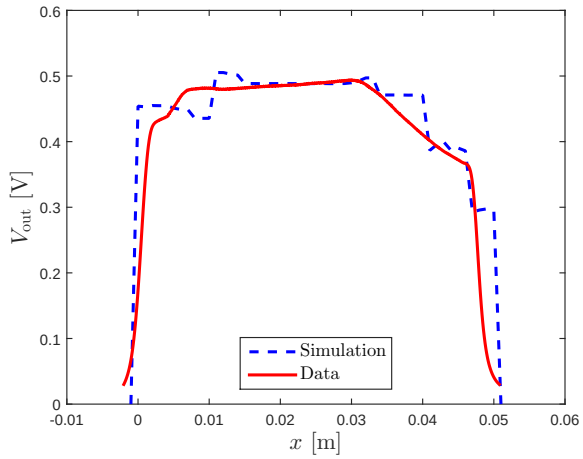

(a) Plot of the output voltage as function of the skate's length together with the according prediction. The prediction is multiplied with a factor 3.2 to correct for the magnitude of the signal. Note that the prediction has 'shoulders', and these 'shoulders' are predicted at the right locations along the skate.

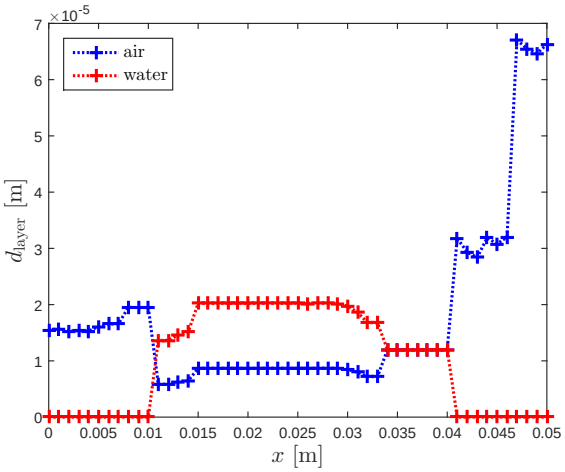

(b) Plot of the composition of the cavity between the skate and the ice layer. In this simulation this cavity is partially filled with air, partially filled with water. All water is simulated around the center (see table 5.2.)

Figure 5.21: *Simulation of a measurement consisting of the output voltage of the system averaged over ten forth passages (being passages 90 to 100). $v_{skate} = 50$ mm/s, $p = 1.5$ bar, experiment conducted at electrode 10. In this simulation water and ice are present. The prediction fits the data better than in the case without ice and water in the cavity.*

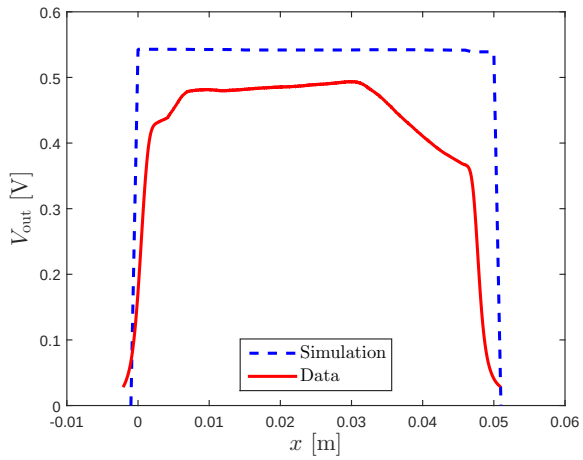

(a) Plot of the output voltage as function of the skate's length together with the according prediction. The prediction is multiplied with a factor 2.8 to correct for the magnitude of the signal. The prediction does not fit the data at all. The 'shoulders' are no longer present.

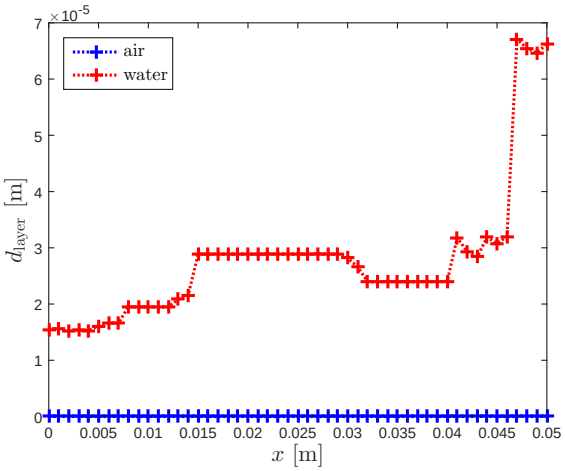

(b) Plot of the composition of the cavity between the skate and the ice layer. In this simulation the cavity is filled only with water.

Figure 5.22: *Simulation of a measurement consisting of the output voltage of the system averaged over ten forth passages (being passages 90 to 100). $v_{skate} = 50$ mm/s, $p = 1.5$ bar, experiment conducted at electrode 10. In this simulation only water and ice are present*

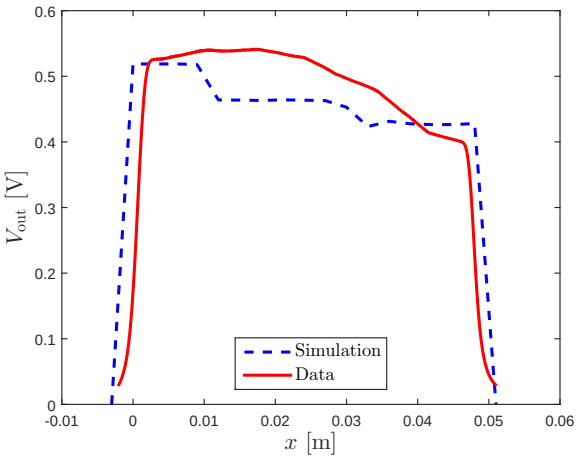

(a) *Plot of the output voltage as function of the skate's length together with the according prediction. The prediction is multiplied with a factor 2.8 to correct for the magnitude of the signal. The prediction does fit the general shape of the data. The 'shoulders' are not present at either the measured data or the prediction.*

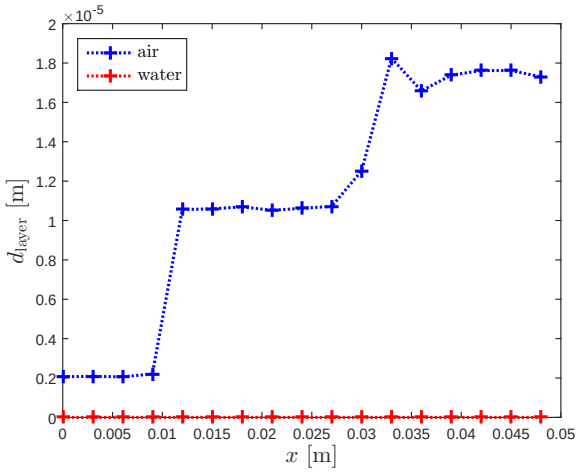

(b) *Plot of the composition of the cavity between the skate and the ice layer. In this case this cavity is filled only with air.*

Figure 5.23: *Simulation of a measurement consisting of the output voltage of the system averaged over ten forth passages (being the first ten passages). $v_{skate} = 50$ mm/s, $p = 0.3$ bar, experiment conducted at electrode 10. In this simulation only air and ice are present*

Table 5.3: *The way the water is distributed over the cavity between the skate and the ice. The columns have the same meaning in table 5.1. These values are used in making the simulation of figure 5.24.*

Part of the skate's length (x)	**Percentage of cavity's height filled with water**
From 0 mm to 7.5 mm	0% water
From 7.5 mm to 25 mm	100% water
From 25 mm to 37.5 mm	50% water
From 35.7 mm to 50 mm	0% water

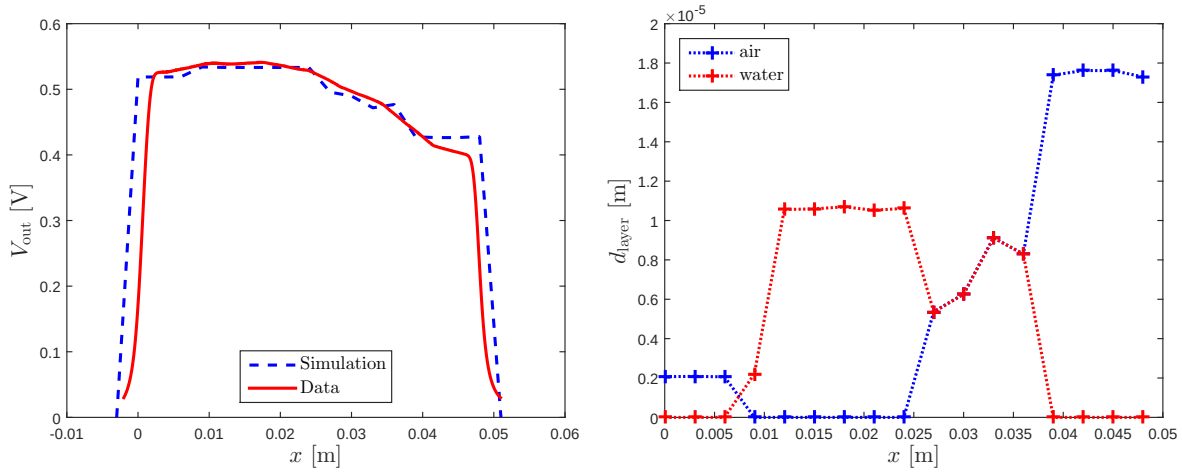

(a) *Plot of the output voltage as function of the skate's length together with the according prediction. The prediction is multiplied with a factor 2.8 to correct for the magnitude of the signal. The prediction does fit the data. The 'shoulders' are not present at either the measured data or the prediction.*

(b) *Plot of the composition of the cavity between the skate and the ice layer. In this case this cavity is partially filled with air, partially filled with water. Almost all water is present around the center (see table 5.3.)*

Figure 5.24: *Simulation of a measurement consisting of the output voltage of the system averaged over ten forth passages (being the first ten passages). $v_{skate} = 50$ mm/s, $p = 0.3$ bar, experiment conducted at electrode 10. In this simulation air, water and ice are present*

5.5.2 Discussion of the usage of *AirLayerSkate.m*

When comparing the results of figure 5.19 to 5.22 it becomes immediately clear that a simulation based upon both water and air present in the cavity between the skate and the ice yields the best result. The water is in this case simulated around the center of the skate.
Most importantly, while comparing 5.19 and figure 5.22 can be concluded that filling the cavity with only water or only with air, the prediction does not fit, this would mean that these extreme situations are not very likely. However, the model is not complete. Moreover, almost all the data is scaled by multiplying with a constant (see discussion of the frequency sweep data; section 5.1.2). This means no hard conclusions can be made about the presence of a water layer. However, the shape of the simulation indicates some water is present in the cavity.

The origin of the 'shoulders' will now be discussed. Since the characteristic kinks in the prediction of figure 5.19 exist and no kinks or 'shoulders' exist in the prediction of figure 5.22, the origin of the shoulders and the location along the skate's length seems to lie in the height profile of the ice layer.
However, the eventual shape of the shoulders seems to be determined by water present in the cavity. This shape seems to be dominated by the water around the center which first presumably sticks to the skate, due to capillary forces, and sequentially detaches from the skate to be refrozen. This can be observed[13] in figure 5.26, together with the

[13]N.B.: since the contents of the cavity can not be verified, the color is 'pimpelpaars met een goud

model hypothesized by Van der Reep in figure 5.25.

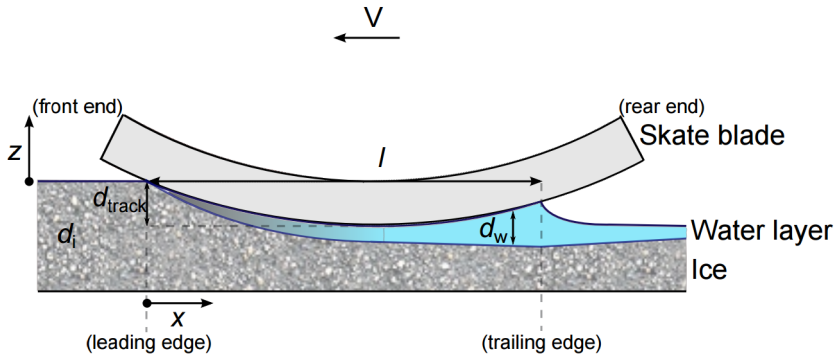

Figure 5.25: *A schematic representation of the water layer under the skate, as hypothesised by Van der Reep. The ice is melted before the center of the skate is present under the skate, sticks to the skate and detaches from the skate. Figure kindly supplied by Van der Reep [3].*

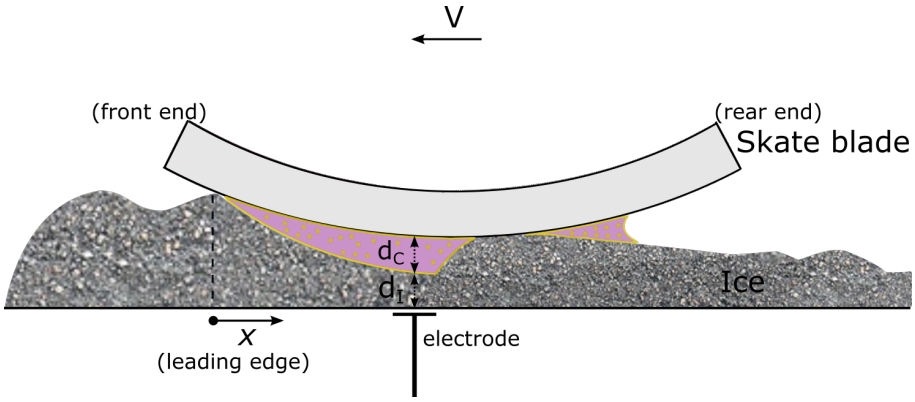

Figure 5.26: *A schematic representation of the proposed current situation under the skate. The skate rests on multiple points, so a cavity is formed between the skate and the ice. This cavity can be filled with water or gas. Since it is not possible to conclude what the contents of the cavity are, it is indicated in purple (see footnote 15 of this chapter). The electrode, the ice thickness (d_I) and the cavity's height (d_C) are depicted. This figure is an adaptation of figure 5.25.*

Striking is that in both measurements discussed more water is simulated before the center, than behind the center of the skate. This would mean a pocket of water is present before the center of the skate. This could be thought of as water that is being plowed forward by the skate. This was already hypothesized by Fennet (see [5]).

When comparing the measurements of figure 5.20 and figure 5.21, we see that the presence of the layer of ice is important of the prediction of the signal. In the case of the presence of ice the influence of water on the signal is less strong, and less water is needed to produce a good prediction. This can be seen in comparing table 5.1 and table 5.2. This influence on the ice layer is not surprising and can be seen in eq. 3.5 where the transfer function and the sample capacitance are related by the reciprocal of a summation of the individual capacitances of the mediums in the sample.

randje' (purple with a golden edge) as 'de boze heks' would say.

Data containing no 'shoulders' is predicted as well. In figure 5.23 can be seen that the characteristic kinks, that are present in the prediction of figure 5.19, are missing in the case of absent 'shoulders' in the measured data. This is further evidence that the shoulders are caused by the structure of the ice.
When the water is added to the simulation, in a similar way as in the simulation of figure 5.22, still no 'shoulders' are visible and the data is fitted better (see figure 5.24). This supports the hypothesis that the location and presence of the 'shoulders' is caused by the ice layer structure and the exact shape of the voltage peak is dominated by the presence of water in the cavity between the ice and the skate.

Further evidence for the cavity can be found when calculating the amount of cavity height is reduced by the skate pressing on the ice. For calculating this reduced height (ΔL) we use:

$$\Delta L = \frac{FL_0}{EA_0} = \frac{FL_0}{Ex_{\text{contact}}w} \tag{5.1}$$

Here F is the force applied on the skate, L_0, the initial height of the ice layer, E the Young's modulus of the ice and A_0 the contact area of the skate and the ice. This last parameter is equal to the product of the contact length (x_{contact}) and the width of the skate (w).
After using the data of figure 5.18(b) (typical condition of the skate on the ice) it was found that $x_{\text{contact}} = 1$ cm. Combined with the estimate $L_0 = 350$ μm, $E = 9$ GPa [22], $w = 1.1$ mm and $F = 16.95$ N this yields:

$$\Delta L = 60 \text{ nm} \tag{5.2}$$

This is much lower than the cavity's height, which means there exists a cavity between the ice and the skate.

The factor used to make the data fit can be thought of as an offset voltage due system properties already discussed in section 5.1.2. These properties are unexplained effects in the electric properties of the sample. This needs to be modeled in the future of the skating project. For now, only the general shape of the simulation can be compared.

Since the magnitude of output voltage of the signal can not be accurately be predicted, conclusions about the magnitude of the thickness of the water layer can not be made[14]. Further research must be done to make conclusions.

[14]The water layer thickness exceeds the maximum thickness found in chapter 2.

Chapter 6

Conclusion and outlook

This chapter will give an overview of the most important conclusions made in chapter 5, followed by some minor ones. This chapter will conclude with some recommendations for future research.

The main conclusions can be summed up as:
The thickness variations in the ice layer are larger than expected. These variations are a factor 20 larger than height variations on the old skate track. This is reduced on the new skate track to a factor 5. Still, this is too large to prevent the formation of cavities between the ice and the skate at the location of the electrode. To make conclusions about the presumed water layer directly under the skate, this cavity must be absent. This must be done by making the ice layer more flat.
The nature of the cavity is studied. No hard conclusions can be made, because the model used in making the predictions is incomplete. However the shape of the measured data is fitted better when in the simulations the cavity was partially filled with water. In the simulations the water was present around the center of the skate.
The presence and the location of the 'shoulders' in the voltage peaks seem have their origin in the distribution of bumps in the ice layer. Moreover, the eventual shape of the shoulders seems to be dominated by the presence of water. However, this hypothesis needs further proof since the model is incomplete.

Minor conclusions are: Sweep data only fits in the case of a direct contact when the skate is in direct contact with the ice. During frequency sweeps with an air layer as sample, the predictions fit after multiplying with a constant. The sweep in the case of an ice sample does not fit in the low frequency range. This can be solved by changing the dielectric constant of the ice. The dielectric constant of ice is depending on the exact circumstances under which the ice is grown; this legalizes the changing of the dielectric constant. The conclusion is that a theoretical part is missing in describing the electrical properties of the sample. The noise signal is predicted with accuracy.
When using the program Compare_signal_characteristics.m it is found that the maximum of the voltage curves change in location along the skate's length, when the number of passes increase. The magnitude of the maximum increases relatively quick in the first measurements. This rate slowed down in later measurements. This means there are bumps in the ice which disappear. The bumps have increasing diameter, when the section is performed deeper in the ice layer. This was confirmed by the dial

gauge data. The process by which the bumps disappear is not yet specified.

Recommendations can be made on several points.
Firstly, and most importantly, The ice surface must be made more flat to study the nature of presumed lubrication layer. This can be done by making the surface of the skate track more hydrophillic than achieved with mica. Moreover, this can be done as well by making a Zamboni-like system which flattens the ice after freezing. An assesment of the height variations of naturally grown ice, as well as ice grown in an ice skating rink are in order.
The settings of Set-up must be tweaked further to achieve better fits in both sweep and noise data. Furthermore, a new piece of theory must be added to Set-up.m to better model the electric interactions in the sample and explain the offset found in sweep data.
To make better conclusions the gauge dial data needs to be more reliable. This could be even done by replacing it with a device which probes with more precision. An optical method which uses interference could be an option. This new technique should be used in the direction perpendicular to the skating track as well as in the regular direction to acquire more insights in the track formation during the passing of the skate.
Definitely, the new force sensor must be used. This is useful to relate the nature of the ice layer and the capacitive data to a friction coefficient. Better temperature measurements must be done as well to better study the influence of frictional heating. These can be incorporated in the ice layer and on the skate.
Finally, the program AirLayerSkate.m must be upgraded to contain the compression of the ice layer due to the pressure on the skate, as well as a model for the inertia of the skate and the friction in the screw connecting the skate to the sensor. This later model will make sure that the flipping motion over the top of a bump is done realistic in the simulation. In this model the refreezing of possible water, must be accounted for.

Work on the skating project will continue. This means that eventually the mystery of the slipperiness of ice will be resolved. Then 430 years after the birth of Hendrik Avercamp, the orange dressed skating fans can be told why the skaters for whom they are so enthusiastic can actually skate.

Acknowledgments

In this chapter I would like to thank a few people important in making this thesis. Firstly, I want to thank my direct supervisor Tom van der Reep for the many insights and help when I was a bit lost in the project. Secondly I want to thank the university's back-up departments, especially Raymond Khoeler (from the ELD) and Gert Koning (from the FMD) for their direct input on the skating project. Finally, I would like to thank all the members of the Interface Physics group, especially my roommates Ian, Queeny, Mathijs and Oliver, for the help and the tremendous time I have had this year.

References

[1] Wikipedia, "lijst van de snelste ijsbanen van nederland," accessed: http://nl.wikipedia.org/wiki/Lijst_van_de_snelste_ijsbanen_van_Nederland, 09-06-2015.

[2] J. van de Vis, "Towards measuring the water layer thickness during ice skating," 2013, batchelors's thesis, Leiden University.

[3] T. H. A. van der Reep, "Why skates skate," 2014, master's thesis, Leiden University.

[4] M. Zuiddam, "Towards calculating the ice, water and air thickness under a blade during ice skating," 2014, batchelors's thesis, Leiden University.

[5] N. Fennet, "Why skates skate," 2015, batchelors's thesis, Leiden University.

[6] R. Rosenberg, "Why is ice slippery?" *Physics Today*, 2005.

[7] J. Joly, *sci. proc. R. Soc. Dublin New Series*, vol. 5, p. 453, 1886.

[8] J. Thomsom, "Theoretical considerations on the effect of pressure in lowering the freezing point of water," *Cambridge and Dublin Math. J.*, vol. 11, pp. 248–255, 1850.

[9] F. Bowden and T. Hughes, "The mechanism of sliding on ice an snow," *Proc. R. Soc. London, Ser. A*, vol. 172, pp. 280–298, 1939.

[10] S. C. Colbeck, L. Najarian, and H. B. Smith, "Sliding temperatures of ice skates," *American Journal of Physics*, vol. 65, no. 6", pp. 488–492, 1997.

[11] A. Mills, *Phys. Educ.*, vol. 43, p. 392, 2008.

[12] T. Ikeda-Fukazawa and K. Kawamura, "Molecular-dynamics studies of surface of ice ih." *J. Chem. Phys.*, vol. 120, pp. 1395 – 1401, 2004.

[13] T. H. McConica, "Sliding on ice and snow," *Report to the Office of the Quartermaster General, US Army*, 1950.

[14] E. R. Pounder, J. A. Jacobs, and J. T. Wilson, *Physics of ice*. Pergamon Press, 1965.

[15] C. D. Niven, "A proposed mechanism for ice friction," *n Can. J. Phys.*, vol. 37, p. 247–55, 1959.

[16] K. Tusima, "Adhesion theory for low friction on ice," *New Tribological Ways, Dr. Taher Ghrib (Ed.)*, vol. 37, p. 247–55, 2011.

[17] *FAST* 2.0 *derivation and new analysis of a hydrodynamic model of speed skate ice friction*. ISOPE, June 2011.

[18] E. Lozowski and K. Szilder, "Derivation and new analysis of a hydrodynamic model of speed skate ice friction," *IJOPE*, vol. 23, pp. 104–111, 2013.

[19] E. Lozowski, K. Szilder, and S. Maw, "A model of ice friction for a speed skate blade," *Sports Eng.*, vol. 16, pp. 239–253, 2013.

[20] T. instruments, "Opa656," December 2008.

[21] H. Dosch, A. Lied, and J. Bilgram, "Glancing-angle x-ray scattering studies of the premelting of ice surfaces," *Surface Science*, vol. 327, no. 1–2, pp. 145 – 164, 1995.

[22] *WHAT IS THE YOUNG'S MODULUS OF ICE?* Dept. Earth and Space Sciences, University of California Los Angeles, 2004.

Appendix A

Lock-in Manual for skating

A.1 The lock-in

The Lock-in amplifier is a device which amplifies a signal at a certain reference frequency. It can find the root mean square amplitude (in Volt; root mean squared) and the phase (in degrees) of the signal and works on the basis of orthogonality of sinusoidal signals. In the lock-in the output (or carrier) signal is mixed with the input signal, this gives a near-DC voltage. This near DC voltage contains information about the amplitude of the signal and the phase of the signal. After mixing the signal is filtered with a low-pass filter to ensure no unwanted higher frequency signals. Because you use a reference signal it is necessary to know the frequency at which you expect your signal. However this drawback is opposed by the fact that an lock-in amplifier can measure signals a million times higher than the noise level.

For more information on how a lock-in works, reading the Wikipedia-page can be useful:

`http://en.wikipedia.org/wiki/Lock-in_amplifier`

A.2 Our set-up

Our set-up uses the Zurich Instruments HF2LI Lock-in Amplifier, which is connected to the computer using a USB 2.0 connection. It is powered by line voltage (230V, AC) and entirely controlled using the supplemented computer program.

A.2.1 The Amplifier and the Connection

Figure A.1 shows the lock-in used in the skating set-up. Parts 1 and 2 are inputs for processing data coming from the skate. Parts 3 and 4 can be used for generating a signal to send to the skate. Figure A.2 shows how the BNC cables must be connected for measurement. The second output signal is drawn as coming from the lock-in,

Figure A.1: *The lock-in of our set-up. Parts 1 en 2 are inputs, parts 3 en 4 transfer output signals.*

though it is also possible to use a function generator instead[1]. As can be seen from figure A.2 the two input signals are added and afterwords the signal is transferred to the ice skate.

After modulation of the signal in the skate, the signal is carried to the lock-in's input. Here it is processed. The raw signal is connected to both inputs; this is done by a BNC splitter.

When using multiple lock-ins (for measuring at more than two vias, or measuring two signals at two different vias) the outputs must be linked subsequently as indicated in figure A.2. Besides the signal must be split (in four cables) and connected to all four inputs.

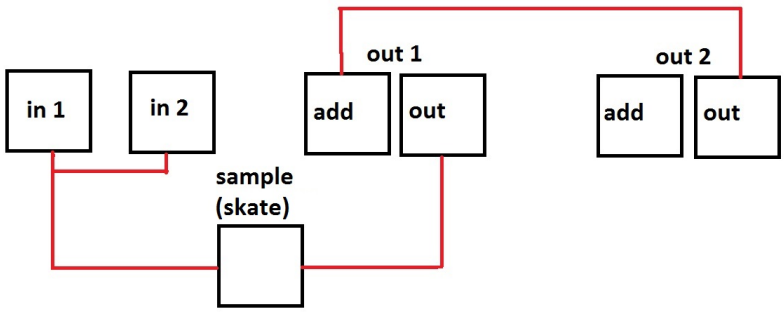

Figure A.2: *The way a single lock-in needs to be connected for the skating project. parts 'in 1' and 'in 2' respectively coincide with parts 1 and 2 of figure A.1. The parts 'out 1' and 'out 2' do so with parts 3 and 4 of figure A.1. The red lines indicate BNC cables.*

A.2.2 The Software

The Zurich Instruments is completely buttonless and all settings are installable using the software. This section gives an overview of the software.

[1]N.B.: If using a Function generator, make sure to properly sync the two devices. This is done by a BNC cable connection between the Sync-port of the function generator and the DIO 0 (or 1) input on the back of the lock-in. In the software the reference must be adjusted to DIO 0 (or 1). See section 2.2.1 for further explanation.

Main screen

In figure A.3 we see the main screen of the lock-in software. We see two rows of settings corresponding to input channel 1 and input channel 2 (parts 1 and 2 in figure A.1 and A.2). I will discuss these settings from left to right.

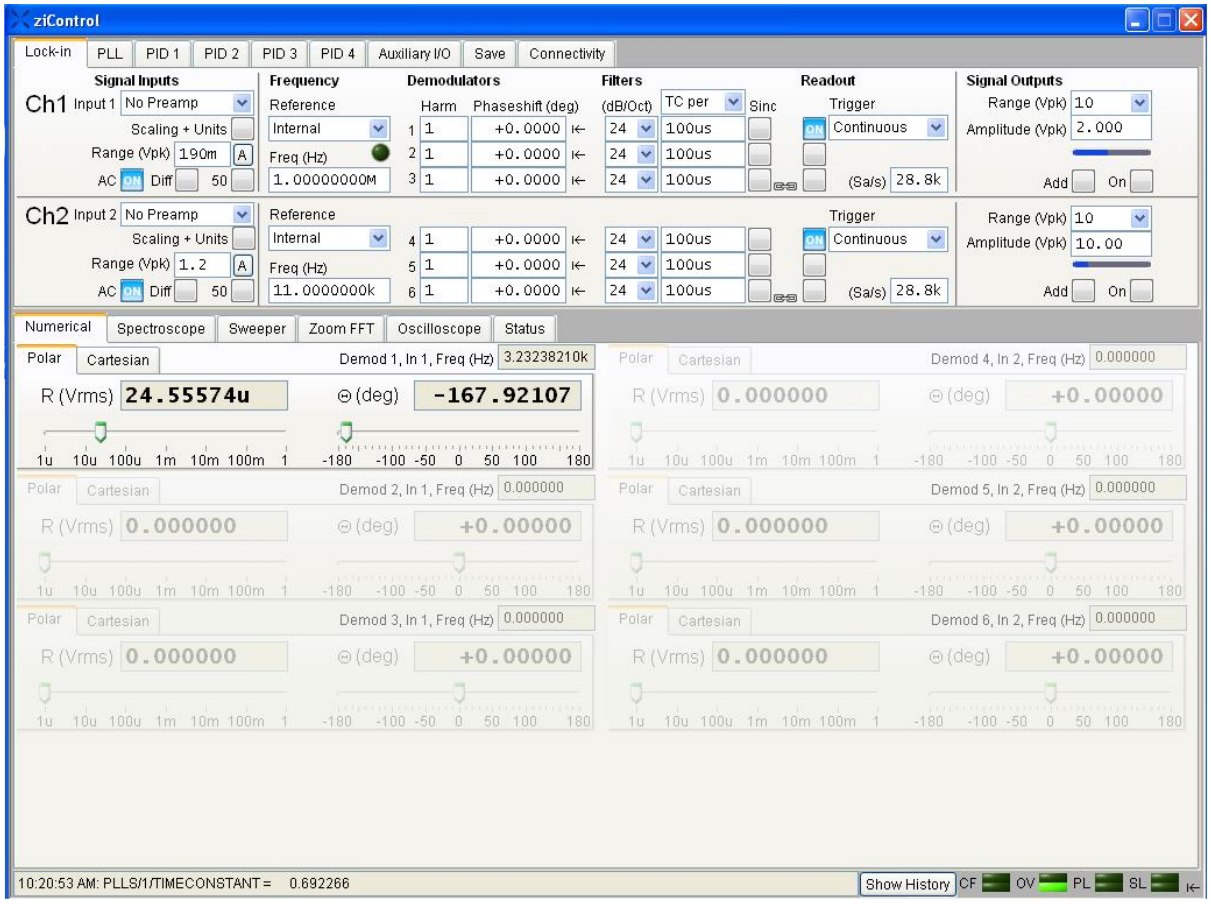

Figure A.3: *The main screen of the Lock-in software. From here we can set all settings concerning the signal*

to switch on an input, put 'AC' on. This setting needs to be on 'on' to measure. The 'Diff' setting should be 'off' to reduce noise. Next is the range (of the input signal). The range needs to be high enough to measure the signal amplitude[2]. this can be accounted for my setting the range to the input signal amplitude. Though the noise level is lower if the range is so too. The 'A' button next to the range sets the range to two times higher than the maximum amplitude registered in the last few seconds.

After this we have the reference frequency; this is the reference at which the rms amplitude is measured. For the skating experiment the reference needs to be internal for signals generated by the lock-in and DIO 0 (or 1, whatever connection is used during building the set-up) for externally generated signals (for example using a signal generator, see subsection 2.1). The frequency needs to be set to the frequency the user wants as output frequency[3].

[2]N.B.: k=10^3, M= 10^6, u= 10^{-6}, n=10^{-9}.
[3]This is done automatically if the reference is set to DIO 0 (or 1)

The filters options give a timeconstant and a slope (in db/oct). These settings, as discussed in section 1, determine the way the signal is filtered after mixing. The time constant determines the lagging behind of the incoming signal. If this time setting is set lower, the lock-in can detect smaller variations in the time domain, but the precision of this detection is less. Whereas if the time setting is set higher, the lock-in amplifier has more time to average the signal so the precision is higher, but it lacks the speed to process small variations in the signal.

The option readout is simply if the input channel is on. To receive any signal any channel one wants to measure must be set to 'on'. The trigger must be set to continuous.

The last option on the main screen is the amplitude output signal[4]. To sent the the signal to the skate, simply check the box 'on'. If a second signal, from the lock-in or a function generator, is added, the box 'add' must be on as well. If it is desired to set the output signal on the lock-in higher, the signal must be adjusted to the maximum range before adjusting the range. This way an electrical overload is avoided.

As can be seen in figure A.3 below the main settings there are tabs. the main tab is 'Numerical'. here the amplitude and phase of the signal can be seen. It is possible to switch to a Cartesian representation of the input signal. On the bottom right corner of the main screen a few indicator lights can be seen (four sets of two). The middle two sets are important. If a top light is on, the error indicated is happening right now, if the bottom light is on, the error happened some time before. The bottom lamps can be reset by clicking the arrow sign right of the lamps. The second lamp means overload; the input signal is higher than the set range. This can be undone by setting the range higher (for example to the input amplitude). The third lamp indicates signal loss, due to a to high sampling rate. This can be accounted for by setting the sampling rate down or turning the oscilloscope off.

The Oscilloscope

The oscilloscope function can be found on the lower row of tabs on the main screen, as indicated in figure A.4. To run the oscilloscope click 'Run'. Under 'Run' the desired input can be selected, together with the sampling rate. The trigger must be set to continuous, just as on the main screen. The 'hold off' can be set lower to produce the FFT of the signal faster if the signal rate is high.

The sampling rate in this case determines the highest frequency visible on the FFT. A higher sampling rate means a frequencies on the FFT but unreliable signals in the low frequency domain. To view lower frequent signals the sampling frequency can be set lower.

The FFT graph is important for looking into the noise spectrum of the signal. The averaging is set to 'RMS averaging', as it should be. The averaging is slow if the number of iterations is higher, but the FFT will be more smooth. The recommended setting is 100 for normal usage, 200 or more for saving data and 20 for higher sampling rates and low hold-off.

[4]N.B.: This output is not a rms amplitude.

If the scales are adjusted to manual the user can change the window of the FFT by clicking on the numbers on the axis of the graph and overwriting with the desired number[5]. For easy processing the x-scale should be logarithmic and the y-scale linear.

To save data from the FFT graph, right-click the FFT graph, select 'export data' and finally click 'export data to excel'[6]

A last important remark about the oscilloscope is to turn it off before doing a measurement. This makes sure no data loss will occur.

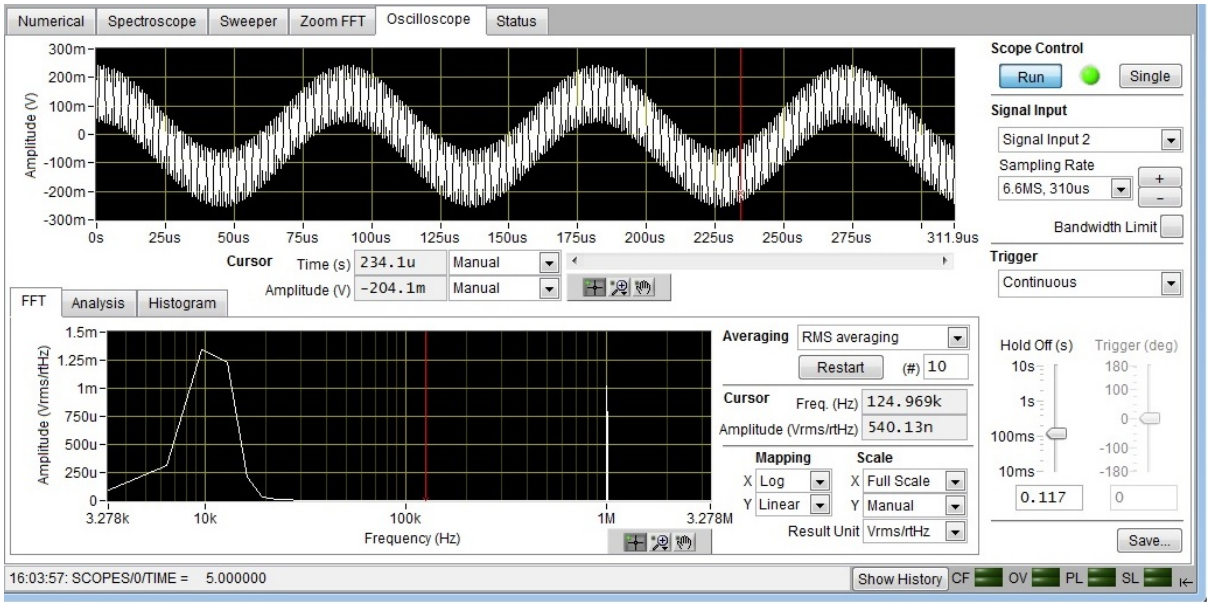

Figure A.4: *The oscilloscope of the Lock-in. Here depicted while the signal is turned 'on'. The top graph is the incoming signal, the lower is the FFT of the signal.*

The Sweeper

In figure A.5 the sweep function of the lock-in can be seen. It is reached from the main screen and is used for measuring the signal strength at various reference frequencies.

In the top right corner of figure A.5 the range of the sweeper can be adjusted, as well as the number of measurements to be done. Raise the number of points and the resolution increases however the time to de the sweep does too. The best option for the skating experiment is to use a log-sweep since we use both 11kHz signals and 1MHz signals. The 'Run/Stop' button can be used to start or stop the sweep.

To save the data of the sweep simply hit 'Save as...' and save the data.

[5] Again we have: k=10^3, M= 10^6, u= 10^{-6}, n=10^{-9}.

[6] N.B.: This function exports the data with letters as powers of ten (u= 10^{-6} etc.). Be sure to use the replace function of excel to change this before processing the data further, as well as deleting the first row of the data (names of the axis). After this save the file as '.csv'-file.

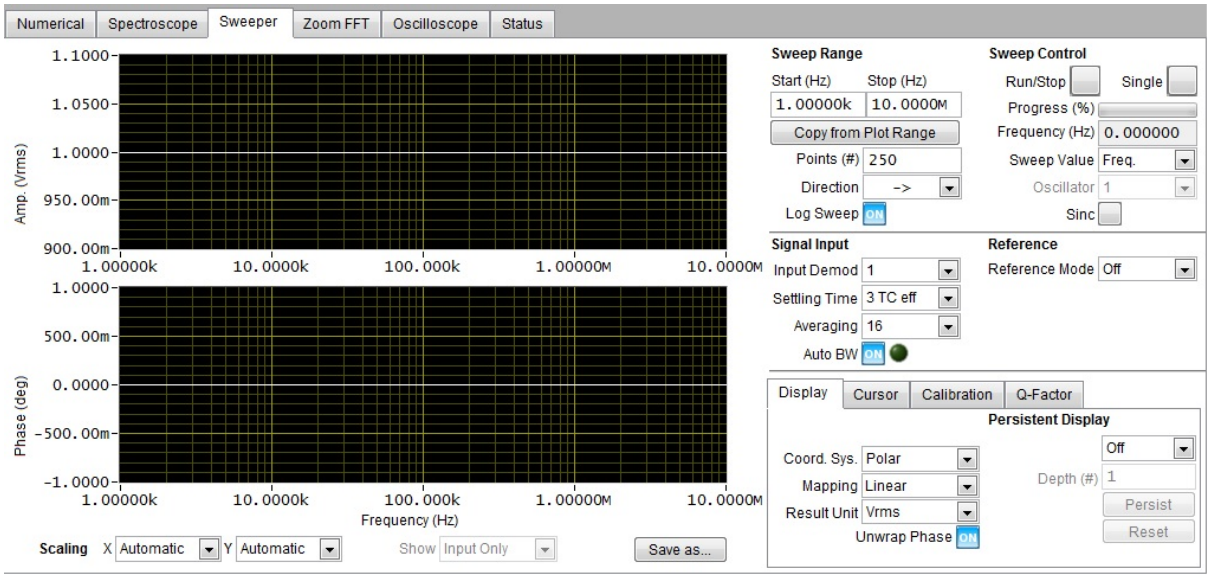

Figure A.5: *The sweeper of the lock-in is used for measuring the output signal at various reference frequencies*

Saving Data

Figure A.6 shows the saving function of the Lock-in, essential for further processing the data. The function can be found between the top row of tabs on the main screen. When using one lock-in amplifier 'Demod 1' corresponds to channel 1 and 'demod 4' corresponds to channel 2. In the box a directory for the output file can be chosen along with a name for the file. For creating manageable file sizes (this means less time consuming processing) the option 'Binary Save' must be checked on.

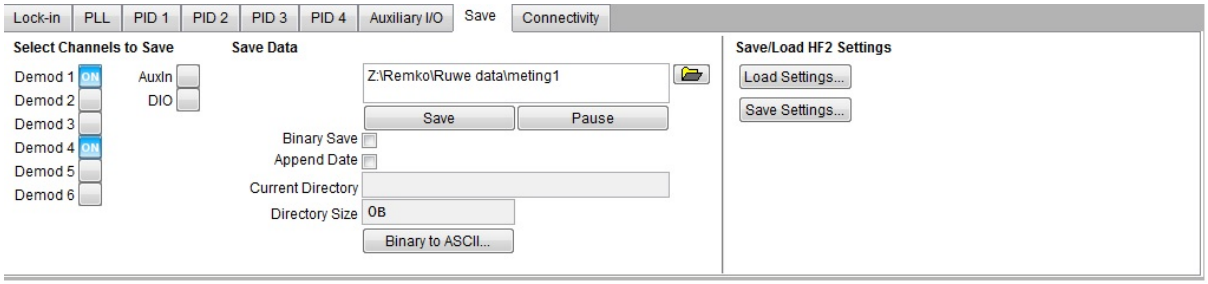

Figure A.6: *The software options for saving the data acquired by the lock-in.*

The procedure of measuring is as follows: First the set-up is prepared and set ready, secondly all software must be set to the right values, thirdly the saving must be started manually, as fourth the measurement is done, finally the saving is stopped manually.